AFRL-RH-WP-TR-2015-0088

HUMAN DECEPTION DETECTION FROM WHOLE BODY MOTION ANALYSIS

David Matsumoto
Hyisung C. Hwang

Humintell, LLC
11165 San Pablo Avenue
PO Box 1304
El Cerrito, CA 94530

Adam M. Fullenkamp
C. Matthew Laurent

Bowling Green State University
C119 Eppler Complex
1001 E. Wooster Street
Bowling Green, OH 43402

DECEMBER 2015
Final Report

Distribution A: Approved for Public Release.

See additional restrictions described on inside pages

AIR FORCE RESEARCH LABORATORY
711TH HUMAN PERFORMANCE WING,
HUMAN EFFECTIVENESS DIRECTORATE,
WRIGHT-PATTERSON AIR FORCE BASE, OH 45433
AIR FORCE MATERIEL COMMAND
UNITED STATES AIR FORCE

NOTICE AND SIGNATURE PAGE

Using Government drawings, specifications, or other data included in this document for any purpose other than Government procurement does not in any way obligate the U.S. Government. The fact that the Government formulated or supplied the drawings, specifications, or other data does not license the holder or any other person or corporation; or convey any rights or permission to manufacture, use, or sell any patented invention that may relate to them.

This report was cleared for public release by the 88th Air Base Wing Public Affairs Office and is available to the general public, including foreign nationals. Copies may be obtained from the Defense Technical Information Center (DTIC) (http://www.dtic.mil).

AFRL-RH-WP-TR-2015-0088 HAS BEEN REVIEWED AND IS APPROVED FOR PUBLICATION IN ACCORDANCE WITH ASSIGNED DISTRIBUTION STATEMENT.

//signature//	//signature//
Timothy S. Webb for Clifford D. Johnson, Work Unit Manager Human Signatures Branch	Louise A. Carter, Chief Human-Centered ISR Division Human Effectiveness Directorate 711th Human Performance Wing Air Force Research Laboratory

This report is published in the interest of scientific and technical information exchange, and its publication does not constitute the Government's approval or disapproval of its ideas or findings.

REPORT DOCUMENTATION PAGE

Form Approved
OMB No. 0704-0188

The public reporting burden for this collection of information is estimated to average 1 hour per response, including the time for reviewing instructions, searching existing data sources, searching existing data sources, gathering and maintaining the data needed, and completing and reviewing the collection of information. Send comments regarding this burden estimate or any other aspect of this collection of information, including suggestions for reducing this burden, to Department of Defense, Washington Headquarters Services, Directorate for Information Operations and Reports (0704-0188), 1215 Jefferson Davis Highway, Suite 1204, Arlington, VA 22202-4302. Respondents should be aware that notwithstanding any other provision of law, no person shall be subject to any penalty for failing to comply with a collection of information if it does not display a currently valid OMB control number. **PLEASE DO NOT RETURN YOUR FORM TO THE ABOVE ADDRESS**.

1. REPORT DATE *(DD-MM-YY)*	2. REPORT TYPE	3. DATES COVERED *(From - To)*
2-12-15	Final	August 2009 – October 2015

4. TITLE AND SUBTITLE
Human Deception Detection from Whole Body Motion Analysis

5a. CONTRACT NUMBER
FA8650-09-D-6949 0002

5b. GRANT NUMBER

5c. PROGRAM ELEMENT NUMBER
61102F

6. AUTHOR(S)
*David Matsumoto
*Hyisung C. Hwang
**Adam M. Fullenkamp
**C. Matthew Laurent

5d. PROJECT NUMBER
2313

5e. TASK NUMBER
B

5f. WORK UNIT NUMBER
H02M 2313B001

7. PERFORMING ORGANIZATION NAME(S) AND ADDRESS(ES)
*Humintell, LLC
11165 San Pablo Avenue
PO Box 1304
El Cerrito, CA 94530

**Bowling Green State University
C119 Eppler Complex
1001 E. Wooster Street
Bowling Green, OH 43402

8. PERFORMING ORGANIZATION REPORT NUMBER
6000-S004

9. SPONSORING/MONITORING AGENCY NAME(S) AND ADDRESS(ES)
Air Force Materiel Command
Air Force Research Laboratory
711th Human Performance Wing
Human Effectiveness Directorate
Human-Centered ISR Division
Human Signatures Branch
Wright-Patterson AFB, OH 45433-7947

10. SPONSORING/MONITORING AGENCY ACRONYM(S)
711 HPW/RHXB

11. SPONSORING/MONITORING AGENCY REPORT NUMBER(S)
AFRL-RH-WP-TR-2015-0088

12. DISTRIBUTION/AVAILABILITY STATEMENT
Distribution A: Approved for Public Release.

13. SUPPLEMENTARY NOTES
Cleared: 88ABW-2016-0244; 25 January 2016. Report contains color.

14. ABSTRACT
This research effort (Year 1, 2, and 3) was intended to discover whole-body motion-based deception signature. The year III effort included the collection of data from an additional 30 participants and focused replication analyses of the new samples based on the original findings from Years 1 and 2. This Year 3 final report summarizes the focused replication analyses of the new samples based on the original findings from Year 1. The findings for the temporal/spatial data from year 3 provided some evidence for the replication of the findings from the Year 1 data using a different sample of individuals from different cultural backgrounds collected at a very different geographical site. It is not clear, however, if the lack of clarity in the findings were due to the geographic site, the mixing of different cultures, ethnicities, and genders in the sample, individual differences, or other factors. The findings do provide evidence that a behavioral signature is likely reliable, but larger, more stratified samples with greater quality control over group and individual difference variables may be necessary to tease apart the effects more carefully in the future.

15. SUBJECT TERMS
Human signatures, deception, security check point, human motion, gait, motion analysis

16. SECURITY CLASSIFICATION OF:			17. LIMITATION OF ABSTRACT:	18. NUMBER OF PAGES	19a. NAME OF RESPONSIBLE PERSON (Monitor)
a. REPORT	b. ABSTRACT	c. THIS PAGE			Cliff Johnson (Timothy Webb)
U	U	U	SAR	55	19b. TELEPHONE NUMBER *(Include Area Code)* (937) 255-6542

Standard Form 298 (Rev. 8-98)
Prescribed by ANSI Std. Z39-18

TABLE OF CONTENTS

LIST OF FIGURE

LIST OF TABLES

1.0 EXECUTIVE SUMMARY

The Statement of Work (SOW) for Year 3 included the collection of data from an additional 30 participants and focused replication analyses of the new samples based on the original findings from Years 1 and 2. The activities for Year 3 were split contractually between Bowling Green State University (BGSU) and Humintell. BGSU was tasked with the collection of data from an additional 30 participants, the submission of data sets for Year 3, and initial analyses. Humintell was tasked with the overall supervision of the conditions for the Year 3 data collection, management of data files, and the focused replication analyses of the new samples based on the original findings from Year 1 (there was no additional data collection in Year 2). This Year 3 Final Report summarizes the focused replication analyses of the new samples based on the original findings from Year 1 conducted by Humintell. Appendix A contains BGSU activities.

The findings for the temporal/spatial data provided some evidence for the replication of the findings from the Year 1 data. It was not clear, however, if the lack of clarity in the findings were due to the geographic site, the mixing of different cultures, ethnicities, and genders in the sample, individual differences, or other factors. The findings did provide evidence that a behavioral signature is likely reliable, but larger, more stratified samples with greater quality control over group and individual difference variables may be necessary to tease apart the effects more carefully in the future.

The findings for the spectral frequency data provided some evidence for the replication of the findings from Year 1. The findings were especially promising for Fmed and F95, as these differentiated liars from truth tellers in both the Baseline vs. Reconnaissance and Baseline vs. Gun Walk analyses.

The findings for the kinematic data provided fairly substantial evidence for the replication of the main effects reported on the kinematic data analyses in Year 1. Although the number of specific variables on which replication was obtained was limited (5), there were a substantial number of variables in the Year 3 data set that produced findings in the same direction for the same body segments in the Year 1 analyses. Additionally, the Year 3 analyses produced significant effects on five new body segments that can potentially discriminate between truth tellers and liars, and should be followed in future research.

Overall, the findings from both Years 1 and 3 provided substantial support for the notion that whole body movements can differentiate truth tellers from liars reliably in a realistic checkpoint scenario that has direct operational relevance. We recommend further tests of the replication and extension of these findings, and for development of assessment capabilities of these whole body movements for potential operational deployment.

Distribution A: Approved for Public Release 88ABW-2016-0244; 25 January 2016

Incorporation of Previously Submitted Reports

This report incorporates by reference the following previously submitted reports:

1) Human Deception Detection from Whole Body Motion Analysis, Year 1 Final report, submitted 17 April 2014 by Bowling Green State University (BGSU) and Humintell
2) Human Deception Detection from Whole Body Motion Analysis, Year 2 Final report, submitted 22 October 2014 by BGSU and Humintell
3) Report of Year 2 Additional Data Analyses, submitted 30 November 2014 by Humintell
4) Additional Report on Year 1 Data: Temporal/Spatial Analyses, submitted by Humintell on 31 December 2014
5) Additional Report on Year 1 Data: Kinematic Analyses, submitted by Humintell on 12 February 2015
6) Additional Analyses Report on Temporal Spatial Data: Gun Condition Differences, submitted by Humintell on 16 April 2015
7) Additional Analyses Report on Spectral Frequencies Data: Gun Condition Differences, submitted by Humintell on 1 May 2015
8) Additional Analyses Report on Kinematics Data: Gun Condition Differences, submitted by Humintell on 28 April 2015
9) Report on Year 3 Data: Temporal/Spatial Analyses, submitted by Humintell on 24 June 2015
10) Report on Year 3 Data: Spectral Frequency Analyses, submitted by Humintell on 9 July 2015
11) Additional Report on Year 3 Data Analyses: Replication of Deception Findings using Kinematic Data, submitted by Humintell on 24 July 2015
12) Human Deception Detection from Whole Body Motion Analysis, Year 3 Final report: Deception recognition analysis from 32, non-US participants, submitted 31 July 2015 by BGSU

Distribution A: Approved for Public Release 88ABW-2016-0244; 25 January 2016

2.0 OVERVIEW OF YEAR 3 REPLICATION ANALYSES

As mentioned above, Humintell's Year 3 obligations were to conduct replication analyses of the original deception findings from Year 1 using the new, Year 3 data samples. In the pages that follow, we separate this report according to the three types of data that were processed and analyzed:

- Temporal/Spatial Data
- Spectral Frequency Data
- Kinematic Data

For each data type we describe briefly the main findings from the initial, Year 1 data analyses that examined whether or not truth tellers and liars could be differentiated according to their whole body movements in the checkpoint scenario. We then present the results of the focused analyses conducted to replicate, or not, the Year 1 deception findings. Because of differences in the nature and size of the samples in Years 1 and 3, we were not as concerned solely with statistical significance in determining replication, but instead used a combination of significance and direction of means to determine partial or full replication of the Year 1 findings.

Also it is important to note that the replication analyses that are presented below are not the entire analyses that were conducted. For example, we computed many overall analyses on the variables, much of which also examined whether whole body movements can differentiate gun vs. no gun carriage (these analyses were reported in additional analyses reports in the Year 1 effort). However, because the specific focus in the Year 3 effort was on the replication of the Year 1 findings, we focus in this final report specifically on those analyses.

Distribution A: Approved for Public Release 88ABW-2016-0244; 25 January 2016

3.0 TEMPORAL/SPATIAL ANALYSES

The purpose of these analyses was to replicate the behavioral signature findings related to veracity vs. deception from the Year 1 data (collected at SFSU) with the Year 3 data (collected at BGSU). This report summarizes the replication analyses we have conducted on the temporal/spatial data from that Year 3 data collection.

To recall, there were four temporal/spatial variables that were generated:

- Cadence (step/min) – frequency of steps per minute
- Step length (cm) – linear distance between alternate heels on subsequent steps
- AVG velocity (cm/min) – mean overground velocity during a gait cycle
- Step width (mm) – mean lateral distance between foot centers within a gait cycle

3.1 REVIEW OF YEAR 1 DATA FINDINGS

We originally computed separate three-way, mixed overall ANOVAs on each of the temporal/spatial variables. The Trial by Veracity interaction was significant for all four variables. We decomposed those interactions by computing two sets of simple interaction contrasts, one comparing Baseline vs. Gun Walk, the other comparing Baseline vs. Reconnaissance. (Because participants knew their condition assignment prior to the Reconnaissance walk, the second interaction contrast also served to test veracity vs. deception.) Across both analyses liars *increased* in their temporal/spatial data at relatively greater rates than did truth tellers. (In the case of step length, liars decreased at lower rates than truth tellers from baseline to gun walk.)

3.2 YEAR 3 DATA FINDINGS

We computed the same interaction contrasts as we did before with the Year 1 data, after computing overall ANOVAs that also included gender as a factor (along with Side, Trial, and Condition; see 150511 temporal spatial 4 ways.xlsx, 150618 temp spatial 3 ways baseline v recon.spv, and 150618 temp spatial 3 ways baseline v gun.spv). Because of the relatively smaller sample size ($N = 32$, but $n_{males} = 16$, and the findings from Year 1 were entirely based on males), we were not as concerned with statistical significance as we were if the means were in the same direction as what was found for Year 1. For the purposes of this report we report a *partial replication* if the direction of the means was in the same direction as those reported in Year 1, and a *full replication* if the direction of the means was in the same direction *and* the finding was statistically significant.

Table 1 summarizes the findings for this interaction contrast, separately for the Baseline vs. Reconnaissance and Baseline vs. Gun Walk analyses. (This was the same analysis plan as used in Year 1 and in the replication efforts below. The reason we did not do the Reconnaissance vs. Gun Walk comparison is because this comparison did not test the deception effect, as both conditions involved deception. Only the two comparisons conducted tested a deception effect.) As can be seen there, there was partial or full replication for six of the eight analyses. The findings were stronger for the Baseline vs Reconnaissance analyses; although the means were in the predicted direction for the Lie Condition in three of the four Baseline vs. Gun Walk analyses, the same mean differences were also observed in the Truth Condition, which qualified those findings.

Distribution A: Approved for Public Release 88ABW-2016-0244; 25 January 2016

Importantly, gender did not interact with any of the Trial by Condition interactions in the overall analyses or in the simple interaction contrast analyses.

3.3 SUMMARY

The findings provided some evidence for the replication of the findings from the Year 1 data using a different sample of individuals from different cultural backgrounds collected at a very different geographical site. It is not clear, however, if the lack of clarity in the findings were due to the geographic site, the mixing of different cultures, ethnicities, and genders in the sample, individual differences, or other factors. The findings do provide evidence that a behavioral signature is likely reliable, but larger, more stratified samples with greater quality control over group and individual difference variables may be necessary to tease apart the effects more carefully in the future.

Table 1. Summary of Replication Analyses for Temporal Spatial Data using Simple Interaction Contrasts, Year 3 Data

Analyses	Variable	Trial by Condition Interaction	Means of the Lie Group in the Predicted Direction?	Replication?	Comment
Baseline vs. Reconnaissance	Cadence	$F(1, 30) = 2.143$, $p = .154$, $\eta_p^2 = .067$	Yes; Baseline < Reconnaissance	Partial	
	Step Length	$F(1, 30) = 8.067$, $p = .008$, $\eta_p^2 = .212$	Yes; Baseline < Reconnaissance	Full	
	Velocity	$F(1, 30) = 5.407$, $p = .027$, $\eta_p^2 = .153$	Yes; Baseline < Reconnaissance	Full	
	Step Width	$F(1, 30) = 9.053$, $p = .005$, $\eta_p^2 = .232$	No	No	
Baseline vs. Gun Walk	Cadence	$F(1, 30) = 3.209$, $p = .083$, $\eta_p^2 = .097$	Yes; Baseline < Gun	Partial	The same difference was observed for truth condition
	Step Length	$F(1, 30) = .036$, $p = .851$, $\eta_p^2 = .001$	Yes; Baseline < Reconnaissance	Partial	The same difference was observed for truth condition
	Velocity	$F(1, 30) = .723$, $p = .402$, $\eta_p^2 = .024$	Yes; Baseline < Reconnaissance	Partial	The same difference was observed for truth condition
	Step Width	$F(1, 30) = .977$, $p = .331$, $\eta_p^2 = .032$	No	No	

Distribution A: Approved for Public Release 88ABW-2016-0244; 25 January 2016

4.0 SPECTRAL FREQUENCY ANALYSES

The purpose of these analyses was to replicate the behavioral signature findings related to veracity vs. deception from the Year 1 data (collected at SFSU) with the Year 3 data (collected at BGSU). This report summarizes the replication analyses we have conducted on the spectral frequencies data from that Year 3 data collection.

To recall, there were four spectral metrics (Fp, Fmed, F95, and Fratio) for each of 13 body segments, The spectral metrics (signatures) denote the frequency of movement, based in time, and capture roughly the degree to which a person's overall motion is slow and fluid with simple oscillations, or jittery and nervous with higher frequency of oscillation. The principal objective in observing whole-body human movement as test participants navigated a simulated security checkpoint was to identify prospective movement features that may serve to indicate when an approaching individual is being deceptive. This, in turn, may indicate that they are concealing some type of contraband item. However, standoff human movement analysis is often limited by confounding variables such as perspective angle, resolution, lighting, and skeletal model fidelity. For these reasons, it is advantageous to identify non-traditional, whole-body movement signatures that exhibit a reduced sensitivity to the aforementioned limiting factors. For this basic research initiative, four movement-based spectral signatures were identified that describe the overall frequency content of human gait as participants approach the security checkpoint (Figure 1). First, the marker tracks data from a given body segment marker cluster were processed to compute a Fast Fourier Transform (FFT) profile. From the FFT profiled associated with each body segment marker cluster, the spectral signatures were derived. The following list provides the spectral variable abbreviations along with a description of the metric:

F_p – the peak frequency response for a given body landmark within a given trial

F_{med} – the median frequency about which the area under the FFT is equal

F_{95} – the frequency at which 95% of the FFT area is below said value

F_{ratio} – the ratio of the 2^{nd} greatest frequency response to the peak frequency

The four metrics described above provide an indication of the prime frequency exhibited in the movement of a body segment, along with information regarding the degree to which the movement frequencies are distributed across the possible range of movement frequencies (based upon sample rate and trial length). It is important to note that, while there is limited frequency information to be obtained from a single motion capture marker, these signatures have been derived for each body segment marker cluster comprising the kinematic model (excluding the pelvis as it is the origin). Segment-specific analyses were anticipated to allow for the development of a more comprehensive and selective concealment/deception prediction model.

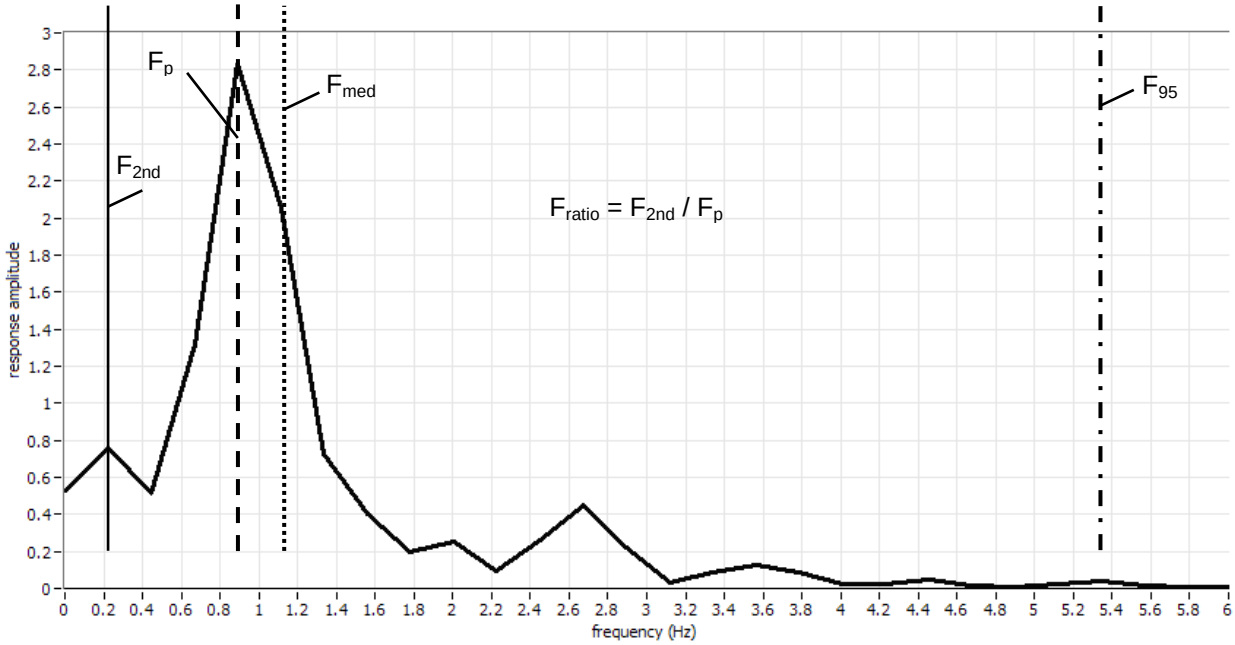

Figure 1. Representative spectral response (FFT) from a single body segment with a depiction of the four frequency signatures (F_p, F_{med}, F_{95}, F_{ratio}) and the intermediate metric (F_{2nd}) required to calculate the ratio of the second largest frequency response to the peak frequency response (F_{ratio}).

The kinematic skeleton model utilized defines 14 anatomical segments. The motion of each body segment was evaluated by tracking the three-dimensional motion of a single cluster of four spherical retro-reflective markers, with the exception of the pelvis cluster, which included only three markers. Of the 14 body segments assessed during motion analyses, the pelvis (denoted as 'PVC' in the raw data) was established as the origin segment for all motion capture trials, which excluded its movement from the frequency metric spreadsheet (Figure 1). As the origin segment, the 3D movement of the pelvis center was subtracted from all other markers in a given trial such that the pelvis center was affixed at the coordinate (0,0,0) and all other markers moved in relation to the pelvis. The visual effect of this origin normalization offers the appearance of what looks like an individual walking on a treadmill. The purpose for this normalization step was to reduce the influence of overground walking velocity and trajectory in the calculation of spectral metrics. While the spectral metrics associated with the remaining 13 body segments are expected to be influenced by overground walking velocity (i.e. segment oscillation frequencies will increase with gait velocity), the relative frequencies across body segments may prove to identify deception independent of gait velocity and trajectory. As the pelvis segment has been described above, the 13 body segments included in the spectral analyses, along with their abbreviations are provided below:

1. HDC – head segment
2. LUA – left upper arm
3. LFA – left forearm
4. LHC – left hand

Distribution A: Approved for Public Release 88ABW-2016-0244; 25 January 2016

5. RUA – right upper arm
6. RFA – right forearm
7. RHC – right hand
8. LTC – left thigh
9. LSC – left shank (i.e. lower leg)
10. LFC – left foot
11. RTC – right thigh
12. RSC – right shank (i.e. lower leg)
13. RFC – right foot

4.1 REVIEW OF YEAR 1 DATA FINDINGS

The main analyses in the Year 1 effort focused on simple interaction contrasts involving Baseline vs. Gun Walk and Baseline vs. Reconnaissance Walk, separately.

Baseline vs. Gun Walk. We computed an initial 3-way mixed ANOVA, using Trial (2: Baseline vs. Gun) and Body Segment (13) as repeated measures factors, and Veracity Condition as a between subjects factor, on the spectral data, separately for each of the spectral metrics. The target effect of interest was the Trial x Veracity Condition interaction.

- For Fp, the interaction was significant, $F(1, 38) = 6.051$, $p = .019$, $\eta_p^2 = .137$. The three-way interaction was not significant, $F(12, 456) = 1.288$, $p = .222$, $\eta_p^2 = .033$. As predicted, spectral frequencies increased from baseline to gun walk for liars, but decreased for truth tellers.
- For Fmed, the interaction was also significant, $F(1, 38) = 4.203$, $p = .047$, $\eta_p^2 = .100$. The three-way interaction was not significant, $F(12, 456) = .346$, $p = .980$, $\eta_p^2 = .009$. As predicted, spectral frequencies increased from baseline to gun walk for liars, but decreased for truth tellers.
- For F95, neither the two-way or three-way interactions was significant, $F(1, 38) = .180$, $p = .674$, $\eta_p^2 = .005$; $F(12, 456) = .546$, $p = .885$, $\eta_p^2 = .014$.
- For Fratio, the interaction was marginally significant, $F(1, 38) = 2.952$, $p = .094$, $\eta_p^2 = .072$. The three-way interaction was not significant, $F(12, 456) = .365$, $p = .975$, $\eta_p^2 = .010$. Once again, as predicted, spectral frequencies increased from baseline to gun walk for liars, but decreased for truth tellers.

These findings provided fairly consistent support for the hypothesis that liars produced significantly higher spectral frequency values than truth tellers when they did the gun walk.

Baseline vs. Reconnaissance. We computed the same three-way analyses as above comparing the Baseline vs. Reconnaissance trials. As above the target effect of interest was the Trial x Veracity Condition interaction.

- For Fp, the interaction was not significant, $F(1, 38) = .421$, $p = .520$, $\eta_p^2 = .011$, but the three-way interaction was, $F(12, 456) = 1.828$, $p = .042$, $\eta_p^2 = .046$. We decomposed the interaction by computing simple interaction contrasts of Trial x Veracity Condition separately for each of the 13 body segments. The simple effects of Left Upper Arm, Left Forearm, and Left Hand were significant, $F(1. 38) = 4.244$, p

Distribution A: Approved for Public Release 88ABW-2016-0244; 25 January 2016

= .046, η_p^2 = .100; F(1. 38) = 4.435, p = .042, η_p^2 = .105; and F(1. 38) = 3.768, p = .060, η_p^2 = .090, respectively. All three contrasts indicated that as predicted, spectral frequencies increased from baseline to reconnaissance walk for liars, but decreased for truth tellers.

- For Fmed, the interaction was marginally significant, F(1, 38) = 3.683, p = .082, η_p^2 = .078. The three-way interaction was also marginally significant, F(12, 456) = 1.572, p = .097, η_p^2 = .040. As predicted, spectral frequencies increased from baseline to gun walk for liars, but decreased for truth tellers.
- For F95, neither the two-way or three-way interactions was significant, F(1, 38) = .878, p = .355, η_p^2 = .023; F(12, 456) = .405, p = .962, η_p^2 = .011.
- For Fratio, neither the two-way or three-way interactions was significant, F(1, 38) = ..400, p = .531, η_p^2 = .010; F(12, 456) = .798, p = .653, η_p^2 = .021.

These findings also provided initial support for the hypothesis that liars produced significantly higher spectral frequency values than truth tellers, even when they did the reconnaissance walk.

4.2 YEAR 3 DATA FINDINGS

We computed the same interaction contrasts as we did before with the Year 1 data, after computing overall ANOVAs that also included gender as a factor (along with Side, Trial, and Condition; see 150526 spectral merged analyses FINAL.xlsx, 150625 spectral overall 5 ways.spv, 150625 spectral baseline v recon interaction contrasts.spv, and 150625 spectral baseline v gun walk interaction contrasts.spv). Because of the relatively smaller sample size (N = 32, but n_{males} = 16, and the findings from Year 1 were entirely based on males), we were not as concerned with statistical significance as we were if the means were in the same direction as what was found for Year 1. For the purposes of this report, we report a *partial replication* if the direction of the means was in the same direction as those reported in Year 1, and a *full replication* if the direction of the means was in the same direction *and* the finding was statistically significant.

Table 2 summarizes the findings for this interaction contrast, separately for the Baseline vs. Reconnaissance and Baseline vs. Gun Walk analyses. As can be seen there, there was partial or full replication for five of the eight analyses. For Baseline vs. Reconnaissance, there was full replication for Fmed and F95; for Baseline vs. Gun Walk, there was full replication for Fp and F95, and partial replication for Fmed. *For all replicated analyses, liars increased in their spectral frequencies for these metrics while truth tellers did not.*

Importantly, gender did not interact with any of the Trial by Condition interactions in the overall analyses or in the simple interaction contrast analyses.

4.3 SUMMARY

The findings provided some evidence for the replication of the findings from the Year 1 data using a different sample of individuals from different cultural backgrounds collected at a very different geographical site. The findings were especially promising for Fmed and F95, as these differentiated liars from truth tellers in both the Baseline vs. Reconnaissance and Baseline vs. Gun Walk analyses.

The lack of clarity of the other findings may have been due to the geographic site, the mixing of different cultures, ethnicities, and genders in the sample, individual differences, or other

factors. Regardless, the findings do provide evidence that a behavioral signature is likely reliable for spectral frequencies.

Table 2. Summary of Replication Analyses for Spectral Frequency Data using Simple Interaction Contrasts, Year 3 Data

Analyses	Spectral Metric	Trial by Condition Interaction	Means of the Lie Group in the Predicted Direction?	Replication?	Comment
Baseline vs. Reconnaissance	Fp	$F(1, 28) = .121$, $p = .731$, $\eta_p^2 = .004$	No	No	
	Fmed	$F(1, 28) = 4.321$, $p = .047$, $\eta_p^2 = .134$	Yes; Baseline < Reconnaissance	Full	
	F95	$F(1, 28) = 4.784$, $p = .037$, $\eta_p^2 = .146$	Yes; Baseline < Reconnaissance	Full	
	Fratio	$F(1, 28) = 1.787$, $p = .192$, $\eta_p^2 = .060$	No	No	
Baseline vs. Gun Walk	Fp	$F(1, 28) = 4.653$, $p = .040$, $\eta_p^2 = .142$	Yes; Baseline < Gun Walk	Full	The same difference was observed for truth condition
	Fmed	$F(1, 28) = .019$, $p = .891$, $\eta_p^2 = .001$	Yes; Baseline < Gun Walk	Partial	The same difference was observed for truth condition
	F95	$F(1, 28) = 3.200$, $p = .084$, $\eta_p^2 = .103$	Yes; Baseline < Gun Walk	Full	
	Fratio	$F(1, 28) = .489$, $p = .490$, $\eta_p^2 = .017$	No	No	

Distribution A: Approved for Public Release 88ABW-2016-0244; 25 January 2016

5.0 KINEMATIC DATA

The purpose of these analyses was to replicate the behavioral signature findings related to veracity vs. deception from the Year 1 data (collected at SFSU) with the Year 3 data (collected at BGSU). This report summarizes the replication analyses we have conducted on the kinematic data from that Year 3 data collection.

5.1 VARIABLE SUMMARY

Joint Articulations and Body Segments. To recall, the kinematic skeleton model utilized for the Year 1 data collection defined 14 anatomical segments. The motions of the segments, either relative to a proximal segment or to the global coordinate system (i.e. room), allowed for the definition of 14 joint movement profiles, along with one global movement profile (pelvis in global). The 3D joint kinematic metrics were calculated by employing an Euler decomposition sequence with a priority of joint flexion/extension (F_E), followed by joint abduction/adduction (Ab_Ad) about an intermediate axis, and finally internal/external (I_E) rotation about the long axis of the distal segment. The joint articulations included in the 3D kinematic analyses, along with brief descriptions of the involved body segments are provided below:

1. Trunk – represents movement of the torso relative to the pelvis
2. Pelvis – represents movement of the pelvis in the global coordinate system
3. Hip – represents movement of the thigh segment relative to the pelvis
4. Knee – represents movement of the lower leg relative to the thigh segment
5. Ankle – represents movement of the foot relative to the lower leg
6. Shoulder – represents movement of the upper arm relative to the torso
7. Elbow – represents movement of the forearm relative to the upper arm
8. Wrist – represents movement of the hand relative to the forearm
9. Head – represents movement of the head relative to the torso

Note: Joint articulation metrics are reported for both the right and left sides of the body for all body segments except head.

3D Kinematic Signature Definitions. The data collection method employed during the Year 3 activities mirrored the Year 1 data collection, and involved the placement and tracking of retro-reflective markers on the body for the 3D kinematic assessment of skeletal motion across the three experimental walking conditions (Baseline, Reconnaissance, and Gun Walk). For the kinematic assessment, we identified four joint angle waveform signatures that described the overall functional performance of each body articulation as participants approached the security checkpoint. The following list provides the 3D kinematic variable abbreviations along with a description of each metric:

movement offset – the mean of joint rotation angles throughout a gait cycle

max angle – the largest joint angle within a gait cycle

min angle – the smallest joint angle within a gait cycle

range of motion – the max angle minus the min angle

The four metrics provide an indication of mean body pose during gait, along with information regarding the joint movement extremes and range. Unlike the spectral signatures, which were analyzed using the raw motion capture files, the 3D kinematic data were filtered using a low-pass, 4th order Butterworth filter with a cutoff frequency of 6Hz prior to analysis. This smoothing process does not compromise the metrics to be obtained from the traditional gait analysis as the purpose of these metrics was to observe differences in movement technique not associated with movement velocity or frequencies.

Thus, for each body segment, there were 3 types of joint articulations (I_E, F_E, and Ab_Ad) x 4 types of signature definitions (Movement Offset, Max Angle, Min Angle, and Range of Motion) x 2 sides (right and left, except for head).

5.2 REVIEW OF YEAR 1 ANALYSES

A number of overall analyses were computed involving Side, Body Segment, Trial (Baseline vs. Reconnaissance vs. Gun Walk), and Veracity Condition (Truth vs. Lie), separately for the joint articulations and signature definitions. We identified all variables that produced a statistically significant or marginally significant two-way interaction between Trial (Baseline vs. Gun or Reconnaissance Walk) and Veracity Condition, as this was the target interaction to identify differences associated with veracity and deception. The variables that were selected in the two sets of interaction contrast analyses are provided in Table 3, 2nd column.

5.3 YEAR 3 DATA FINDINGS

We computed the same analyses as in Year 1, starting with overall, mixed ANOVAs with Side (2), Trial (3), Veracity Condition (2), and Gender as independent variables, separately for each body segment, joint articulation, and signature definition. (Analyses for head did not include Side as a factor.) Because we were not concerned with statistical significance, given the difference in sample size and composition, for the purposes of the replication, we first identified all significant two-way interactions between Trial and Veracity Condition (see 150709 Kinematic Final Merged analysis summary.xlsx), and then compared the direction of the means in the significant interaction with the direction of the means in the significant effects reported in Year 1.

The results are in Table 3. As mentioned above, the 2nd column lists the variables from the Year 1 Findings that produced significant or marginally significant two-way simple interaction contrasts (Baseline vs. Gun Walk or Baseline vs. Reconnaissance). The 3rd column lists the variables from the Year 3 findings that produced significant or marginally significant two-way overall interactions. The last two columns compare the direction of the means in the Year 3 analyses with the direction of the effects reported previously in the Year 1 findings. The comparison of the direction of the means was still done for findings produced from the Year 3 data on the same body segment but a different signature or joint articulation as the Year 1 data. As can be seen in Table 3, the findings from Year 3 produced a substantial number of replicated effects.

The analyses from Year 3 also produced a number of significant effects for variables that were not significant in Year 1. Please see Table 4. Because these effects did not occur on these body segments in the Year 1 data, they cannot be considered replications, but they do provide additional potential findings that allow for discrimination between truth tellers and liars.

5.4 SUMMARY

The analyses documented fairly substantial evidence for the replication of the main effects reported on the kinematic data analyses in Year 1. Although there were only five variables on which replication was obtained, there were a substantial number of variables in the Year 3 data set that produced findings in the same direction for the same body segments in the Year 1 analyses. Additionally, the Year 3 analyses produced significant effects on five new body segments that can potentially discriminate between truth tellers and liars, and should be followed in future research.

Table 3. Comparison of Findings From Year 1 and Year 3 Kinematic Data Involving Overlapping Body Segments

Body Segment	Variables from Year 1 Findings that Produced Significant or Marginally Significant Two-Way Simple Interaction Contrasts (Baseline vs. Gun Walk or Baseline vs. Reconnaissance)	Variables from Year 3 Findings that Produced Significant or Marginally Significant Two-Way Overall Interaction	Same Direction of Difference – Baseline vs. Gun Walk from Year 1?	Same Direction of Difference – Baseline vs. Reconnaissance from Year 1?
Hip	Hip_Ab_Ad_deg_Min_Angle_deg			
	Hip_F_E_deg_Max_Angle_deg			
	Hip_F_E_deg_Range_of_Motion_deg	Hip_F_E_deg_Range_of_Motion_deg	Yes	Yes
		Hip_F_E_deg_Min_Angle_deg	Yes	Yes
		Hip_Ab_Ad_deg_Max_Angle_deg	Yes	Yes
		Hip_Ab_Ad_deg_Range_of_Motion_deg	Yes	Yes
		Hip_I_E_deg_Min_Angle_deg	Yes	Yes
		Hip_I_E_deg_Range_of_Motion_deg	No	No
Knee	Knee_I_E_deg_Max_Angle_deg	Knee_I_E_deg_Max_Angle_deg	Yes	Yes
	Knee_I_E_deg_Min_Angle_deg			
	Knee_F_E_deg_Range_of_Motion_deg	Knee_F_E_deg_Range_of_Motion_deg	Yes	Yes
	Knee_F_E_deg_Min_Angle_deg			
	Knee_Ab_Ad_deg_Movement_Offset_deg			
		Knee_I_E_deg_Range_of_Motion_deg	NO	Yes
Ankle	Ankle_F_E_deg_Range_of_Motion_deg	Ankle_F_E_deg_Range_of_Motion_deg	Yes	Yes
	Ankle_F_E_deg_Min_Angle_deg	Ankle_F_E_deg_Min_Angle_deg	Yes	Yes
		Ankle_I_E_deg_Max_Angle_deg	Yes	Yes
		Ankle_I_E_deg_Range_of_Motion_deg	No	No
Trunk	Trunk_Ab_Ad_deg_Movement_Offset_deg			
	Trunk_Ab_Ad_deg_Max_Angle_deg			
	Trunk_F_E_deg_Range_of_Motion_deg			
		Trunk_I_E_deg_Range_of_Motion_deg	Yes	Yes
		Trunk_I_E_deg_Max_Angle_deg	Yes	Yes
		Trunk_Ab_Ad_deg_Range_of_Motion_deg	Yes	Yes

Distribution A: Approved for Public Release 88ABW-2016-0244; 25 January 2016

Table 4. Kinematic Variables from Year 3 Data that Produced Significant Two-Way Trial by Veracity Condition Interactions, but were not Significant in Year 1

Variable	Condition		Baseline	Reconnaissance	Gun Walk	Two-Way Interaction				
						df_1	df_2	F	p	η_p^2
Pelvis_I_E_deg_Max_Angle_deg	Truth	M	-5.175	-5.454	-4.619	2	56	2.845	.067	.092
		SE	1.552	1.501	1.440					
	Lie	M	-6.896	-7.124	-5.493					
		SE	1.552	1.501	1.440					
Pelvis_Ab_Ad_deg_Range_of_Motion_deg	Truth	M	9.051	8.940	9.630	2	56	3.196	.048	.102
		SE	.612	.652	.578					
	Lie	M	8.446	8.894	8.933					
		SE	.612	.652	.578					
Shoulder_Ab_Ad_deg_Movement_Offset_deg	Truth	M	7.897	8.242	8.646	2	56	2.846	.067	.092
		SE	.910	.961	.908					
	Lie	M	7.963	8.127	8.129					
		SE	.910	.961	.908					
Wrist_F_E_deg_Max_Angle_deg	Truth	M	-2.337	-2.669	-1.098	2	56	3.387	.041	.108
		SE	2.075	2.042	2.065					
	Lie	M	2.683	3.957	3.721					
		SE	2.075	2.042	2.065					
Elbow_F_E_deg_Movement_Offset_deg	Truth	M	23.348	23.700	24.843	2	56	3.365	.042	.107
		SE	2.083	2.171	2.128					
	Lie	M	23.910	24.518	24.150					
		SE	2.083	2.171	2.128					

Distribution A: Approved for Public Release 88ABW-2016-0244; 25 January 2016

APPENDIX A. BOWLING GREEN STATE UNIVERSITY

Year 3 - Deception recognition analysis from 32, non-U.S. participants
31 July 2015

1. Principal Investigators

a. Adam M. Fullenkamp, Ph.D. / Assistant Professor, Exercise Science Program, Bowling Green State University, 419-372-6929, fullena@bgsu.edu
b. C. Matthew Laurent, Ph.D. / Assistant Professor, Exercise Science Program, Bowling Green State University, 419-372-6904, cmlaure@bgsu.edu
c. David Matsumoto, Ph.D. / Director, Humintell Corp., El Cerrito, CA, 510-912-8741, dmatsumoto@humintell.com
d. Hyisung C. Hwang, Ph.D. / Humintell, El Cerrito, CA, 510-704-1883

2. Associate Investigators

a. Danilo Tolusso/Research Associate, Division of Kinesiology, Bowling Green State University, danilot@bgsu.edu
b. Kaitlyn Kielsmeier/Masters Research Assistant, Division of Kinesiology, Bowling Green State University, kkielsm@bgsu.edu
c. Devansh Shah/Masters Research Assistant, Division of Kinesiology, Bowling Green State University, devshah@bgsu.edu

3. Executive Summary

The purpose of the Year 3 task effort was to analyze the whole-body human movement characteristics of 32 non-U.S. test participants as they navigated a simulated security checkpoint under conditions of truth-telling (i.e. carrying a concealed simulated handgun legally) and deception (i.e. concealing an illegal simulated handgun). It was hypothesized that distinctive whole-body movement cues would allow for the prediction of participants engaged in deception from standoff. An added purpose of the Year 3 effort was to compare the prediction modeling results obtained from a U.S.-born sample (Years 1 & 2 of the 3-year investigation) to the current non-U.S. sample in order to assess the potential for cross-cultural differences in whole-body movement cues of deception. It was hypothesized that whole-body deception cue differences would exist between the U.S.-born and non-U.S. participants samples. This hypothesis stems from existing scientific evidence which demonstrates that there are differences in non-verbal deception cues across different cultural populations.

4. Objective

The objectives for this task order effort included the following: 1.) Conduct gait kinematic recognition simulation and analyses on a dataset of 32, non-U.S. adults in order to establish a predictive model for the recognition of individuals engaged in deception as they approach a simulated entry control point (ECP), 2.) Analyze a set of 3D motion capture data to identify

predictive metrics for the distinction of liars vs. non-liars, 3) Compare the deception prediction performance between samples of U.S.-born and non-U.S. test participants in order to identify potential cross-cultural differences in whole-body deception cues.

5. Challenge

The principal challenge associated with the data collection and analysis effort was to recreate the simulated ECP scenario employed for the Year 1 data collection. Further, the current data collection required the incentivisation of a non-U.S. population with an enculturation varied from that of the U.S.-born population. The effort also involved the comparison of whole-body deception cues between U.S-born and non-U.S. participants samples. The products of this effort include a catalog of novel software utilities, a series of multivariate analyses and logistic regression recognition models, along with the following summary report.

6. Impact

The collection, analysis and comparison of both U.S.-born and non-U.S. ECP navigation may lead to the discovery of a set of culturally-specific (or independent) human movement signatures which predict the likelihood that someone approaching a checkpoint is being deceptive, or concealing some type of contraband item. The ability to identify human deception/concealment from a distance offers security personnel the opportunity to cue in on potential threats prior to their coming within striking distance. Such distance-based assessment techniques may also assist operators in the rapid downselection of potential threats for further inspection, a process that is now conducted exclusively by trained personnel. If it can be demonstrated that whole-body movement cues provide a reliable means of remote deception detection, then such signatures may facilitate the development of novel cuing systems to support ground-based security applications.

7. Simulated Checkpoint Data Collection Method

The Year 3 task involved the collection of motion analysis and standard 2D video data for a set of 32 non-U.S. test participants as they approached a simulated security checkpoint. In order to elicit the genuine emotional response associated with incentivized deception, an initial reward/punishment protocol was designed to apply a level of stakes/significance to the checkpoint navigation process. The following is a summary of the data collection method established for the Year 3 effort. This method followed, as closely as possible, the method prescribed for the Year 1 data collection.

All subjects were provided an informed consent document for their review and signature prior to testing. After all questions and clarifications had been addressed by the investigators, and the subjects had signed the informed consent document, the testing began. Participants completed a basic demographic questionnaire, and personality inventories (Neuroticism-Extraversion-Openness Five Factor Inventory; NEO-FFI), Emotional Expressivity Scale (EES), Self-Monitoring Scale, Social Dominance Orientation Scale, Aggression Scale and Machiavellianism Scale.

Distribution A: Approved for Public Release 88ABW-2016-0244; 25 January 2016

Participants were then asked to don a tank top shirt and jean shorts provided by the investigators. After they had changed into the clothing, a researcher affixed a series of retro-reflective marker to the major joints and body segments of each participant for human movement tracking. Subjects were then taken to an open portion of the lab where the 3D motion capture and 2D Full Motion Video (FMV) cameras had been set up to capture video of them performing a series of walking trials.

For the first series of walking trials, participants were asked to walk at a self-selected pace (i.e., normal gait) across the length of the laboratory space. These walking trials were designated as Baseline walking trials (WK) and each participant performed a minimum of three such trials. Following the WK trials, participants were taken into a room adjoining the lab. With the participant in a separate room, and without line-of-sight to the lab, a research assistant prepared the simulated security checkpoint, which consisted of fake barbed wire covered chain link fencing at the opposite end of the laboratory accompanied by signage consistent with a government checkpoint/installation. Additionally, a research assistant dressed as a checkpoint police officer and assumed the role of the guard at the opening of the checkpoint. The checkpoint guard held a decommissioned, rubberized M4 training gun. While the checkpoint was being assembled, the participants were prepared for the next phase of the experiment. They were informed that they would walk the capture volume two additional times, but during these trials, they would be required to pass through the security checkpoint with the armed guard. They were told that during the first trial, they would not be carrying anything through the checkpoint (this was designated as the Reconnaissance trial [RW]), but that during the second trial they would be asked to carry an inert, Berretta training handgun (this was designated as the Gun trial [GW]). For the experimental condition that involved a participant acting truthfully, they were given a permit to carry the handgun through the checkpoint. For the condition that involved acting deceptively, participants were given a false permit and were asked to illegally carry the gun through the checkpoint. The inclusion of a given test participant in either the Truthful (i.e. gun carried legally) or the Deceptive (i.e. gun concealed illegally) experimental conditions was counterbalanced throughout the test sample.

Prior to beginning the final two walking trials, all participants were shown a video of what would happen if the guard thought that a participant was illegally carrying a weapon through the checkpoint. In the video, a staged participant could be seen being stopped and handcuffed by the checkpoint guard. This scenario was, of course, fictional and no participant was actually stopped as they walked through the checkpoint, regardless of whether they were part of the Truthful or Deceptive condition. However, for the purposes of ecological validity participants were led to believe that such a detention could occur.

After the determination was made for a given participant to engage as either a truthful or deceptive actor, the participants completed one RW trial, where they walked through the guarded checkpoint without the gun in their possession. They were guided by an experimenter to the start position within the lab, and the guard announced “Proceed to the checkpoint” to start the trial. A 2D FMV camera was positioned behind the checkpoint and focused over the shoulder of the guard for the purpose of recording participant facial movement during the checkpoint interaction. Once the participant arrived at the checkpoint the guard would say “Provide identification”. Participants then presented the guard their driver’s license or another form of identification.

Then the guard would say "You are clear to proceed past the checkpoint". The participants then walked through the checkpoint opening and were led by an experimenter back to the room adjoining the lab. For the GW trial, the participants were asked to carry an inert Beretta handgun in the rear waistband of their shorts on the right-hand side. Participants acting truthfully were given a simulated "legal" gun permit, whereas participants acting to deceive were given what they were told was a false permit. The participants then approached the checkpoint in the same manner as the RW trial detailed above. At the checkpoint, the guard asked the participants the following questions after providing identification:

"Is this you?"
"Do you have in your possession anything that you should not be carrying?"
"Are you carrying anything that can be used as a weapon?"
-If yes, "Do you have a permit to carry that weapon?"
-If yes, "May I see the permit?"
-If no, "If I searched you right now would I find any weapon?"
"Proceed through the checkpoint and exit to your right."

Participants were then allowed to pass through the checkpoint. After the completion of the GW, participants walked back to the room adjoining the lab and were asked to fill out a post-session questionnaire asking them about their emotions and deception strategy. Once completed, the participants removed all the markers and changed into their regular clothing. Finally, the participants received their $25 (for those in the non-liar condition) or $50 (for those in the Deception condition) compensation for their participation in the experiment and they were debriefed.

8. Dataset and Analyses

8.1 Participant Demographics

The completed dataset was comprised of 32, mostly college aged, non-U.S. participants (Table 1). Specifically, the sample included 20 Indian participants, two Chinese participants, and one participant from each of Austria, Bali, Bangladesh, Bosnia, Brazil, Indonesia, Nepal, Spain, Sri-Lanka and Taiwan.

Table 1. Demographic results for Year 3 test participants [AVG (SD)]

	Size (n)	Height (cm)	Body Mass (kg)	Age (yrs)	Deceptive Participants (n)	Left Handed Participants (n)
Males	16	171.6 (7.2)	72.3 (8.6)	25.0 (3.6)	8	0
Females	16	157.8 (7.0)	60.1 (9.7)	24.9 (2.2)	8	1

8.2 Spectral Analyses of Motion Capture Data

8.2.1. Motion Capture Spectral Variables Description

The output file for the spectral motion capture analysis was organized according to trial type, spectral metric and body segment. Additionally, in order to facilitate the direct comparison of a given spectral metric within a given body segment across all walking trial conditions, the data were formatted according to Figure 1.

G	H	I	J	K	L	M	N
Age_(yrs)	WK_Fp_HDC	RW_Fp_HDC	GW_Fp_HDC	WK_Fmed_HDC	RW_Fmed_HDC	GW_Fmed_HDC	WK_F95_HDC
23	0.892	0.891	0.222	0.858	0.876	0.813	3.977
21	0.724	0.871	0.633	0.983	1.102	0.930	19.811
24	0.848	0.753	0.299	0.999	0.810	0.890	11.001
19	0.817	0.866	0.877	0.948	1.304	1.162	6.657
23	0.882	0.929	0.712	0.856	0.907	1.214	10.003
22	0.536	0.839	0.222	0.835	0.833	0.728	8.159

Figure 1. Columns H-J depict the peak movement frequency (Fp) for the head segment during each of the three walking trials (Baseline walk [WK], Reconnaissance walk [RW], and Gun walk [GW]).

The following sections will provide a detailed description of the annotation schema established for the experimental trials, body segment parameters and spectral movement signatures.

8.2.2. Trial Type Definitions

The Year 3 data collection involved three different walking trial types. The first walking trial condition was the WK trial. All test participants engaged in four WK trials for which they assumed a self-selected gait velocity. Also, during the WK trials, the simulated entry control point was hidden from the participant's view. The second walking trial type, referred to as the RW, was completed after the entry control area was staged within the lab and participants had watched a priming video which demonstrated that they would be detained if determined to be concealing a contraband item. For the RW condition, participants engaged in only one trial. Finally, participants were given a simulated handgun in a preparation room before engaging in a final walking trial, referred to as the GW trial. As with the RW condition, the GW condition consisted of a single trial. All movement-based signatures were derived for each body segment within each walking trial type and exported to a single Excel spreadsheet (Figure 1). For each

variable within the output spreadsheet, walking condition was annotated using the following abbreviations in the variable name:

WK – referring to a Baseline Walk trial
RW – referring to a Reconnaissance Walk trial
GW – referring to a Gun Walk trial

It should be noted that the movement-based signatures derived for the three-to-four control walking trials for each participant were averaged so that each walk condition for each participant provides a single movement variable for each body segment and variable type.

8.2.3. Movement-Based Spectral Signature Definitions

The principal objective in observing whole-body human movement as test participants navigated a simulated security checkpoint was to identify prospective movement features that may serve to indicate when an approaching individual is being deceptive. This, in turn, may indicate that they are concealing some type of contraband item. However, standoff human movement analysis is often limited by confounding variables such as perspective angle, resolution, lighting, and skeletal model fidelity. For these reasons, it is advantageous to identify non-traditional, whole-body movement signatures that exhibit a reduced sensitivity to the aforementioned limiting factors. For this basic research initiative, four movement-based spectral signatures were identified that describe the overall frequency content of human gait as participants approach the security checkpoint (Figure 2). First, the marker tracks data from a given body segment marker (i.e. mid-segment planar marker) were processed to compute a fast Fourier transform (FFT) profile. From the FFT profiled associated with each body segment marker cluster, the spectral signatures were derived. The following list provides the spectral variable abbreviations along with a description of each metric:

Fp – the peak frequency response for a given body landmark within a given trial
Fmed – the median frequency about which the area under the FFT is equal
F95 – the frequency at which 95% of the FFT area is below said value
Fratio – the ratio of the 2nd greatest frequency response to the peak frequency

The four metrics described above provide an indication of the primary frequencies exhibited in the movement of a body segment, along with information regarding the degree to which the movement frequencies are distributed across the possible range of movement frequencies (based upon sample rate and trial length). It is important to note that, while there is limited frequency information to be obtained from a single body segment, these signatures have been derived for each body segment comprising the kinematic model (excluding the pelvis as it is the origin). Segment-specific analyses were anticipated to allow for the development of a more comprehensive and selective concealment/deception prediction model.

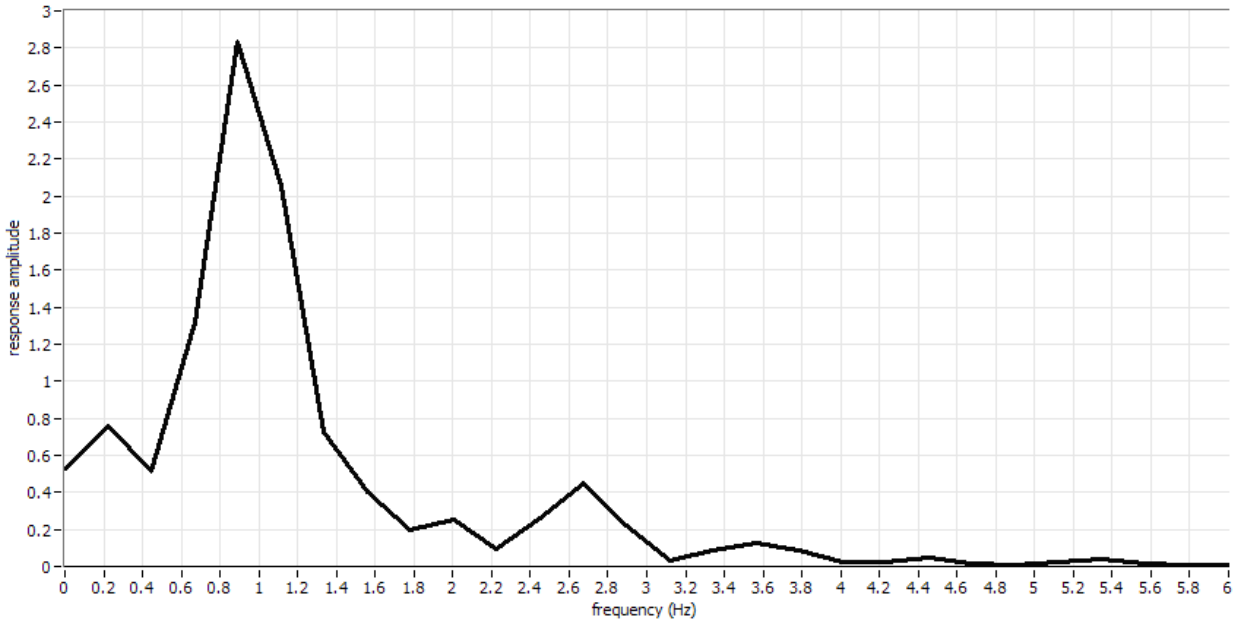

Figure 2. Representative spectral response (FFT) from a single body segment with a depiction of the four spectral signatures (Fp, Fmed, F95, Fratio) and the intermediate metric (F_{2nd}) required to calculate the ratio of the second largest frequency response to the peak frequency response (Fratio).

8.2.4. Annotation of Body Segments

The kinematic skeleton model utilized for the Year 3 data collection defines 14 anatomical segments. The motion of each body segment was evaluated by tracking the three-dimensional motion of a sparse marker configuration of three, spherical retro-reflective markers. Of the 14 body segments assessed during motion analyses, the pelvis (denoted as 'PVC' in the raw data) was established as the origin segment for all motion capture trials, which excluded its movement from the spectral metric spreadsheet (Figure 1). As the origin segment, the 3D movement of the pelvis center was subtracted from all other markers in a given trial such that the pelvis center was affixed at the coordinate (0,0,0) and all other markers moved in relation to the pelvis. The visual effect of this origin normalization offers the appearance of what looks like an individual walking on a treadmill. The purpose for this normalization step was to reduce the influence of overground walking velocity and trajectory in the calculation of spectral metrics. While the spectral metrics associated with the remaining 13 body segments are expected to be influenced by overground walking velocity (i.e. segment oscillation frequencies will increase with gait velocity), the relative frequencies across body segments may serve to identify deception independent of gait velocity and trajectory.

As the pelvis segment has been described above, the 13 body segments included in the spectral analyses, along with their abbreviations are provided below:

1. HDC – head segment
2. LUA – left upper arm
3. LFA – left forearm
4. LHC – left hand
5. RUA – right upper arm
6. RFA – right forearm
7. RHC – right hand
8. LTC – left thigh
9. LSC – left shank (i.e. lower leg)
10. LFC – left foot
11. RTC – right thigh
12. RSC – right shank (i.e. lower leg)
13. RFC – right foot

8.2.5. Variable Labeling in the Spectral Results Spreadsheet

The first seven columns of the spectral results spreadsheet provide the basic demographic and experimental condition data associated with each participant. Below is a listing of the included variables and their definitions:

1. Subject_# - unique subject number ranging from 1001 to 1032
2. Condition_(0-truth,1-lie) – identifies a participant as a truthful participant (denoted with a value of '0') or a deceptive participant (value = 1)
3. Gender_(0-M,1-F) – denotes the gender of a given participant
4. Handedness_(0-Rt,1-Lt) – identifies the handedness of a participant
5. Height_(cm) – identifies participant height in centimeters
6. Weight_(lb) – identifies participant body weight in pounds
7. Age_(yrs) – identifies participant age in years

The remaining metrics reported in the spectral results spreadsheet have been labeled according to walking trial type, spectral metric and body segment, respectively. For example, column L in Figure 1 depicts a variable labeled "RW_Fmed_HDC". This signifies that the variables in this column represent the Fmed variable for the head segment during the RW trial for all participants. Further, the spectral metrics in the spreadsheet have been arranged to facilitate the direct comparison of like metrics associated with like segments across the three walking conditions.

8.3 Traditional 3D Kinematic Analyses of Motion Capture Data

8.3.1. Motion Capture: 3D Kinematic Variables Description

The output file associated with the 3D kinematic motion capture analyses has been organized according to trial type, joint articulation, joint plane movement and kinematic metric. Additionally, the data have been organized with a single gait kinematic metric across all walking trial conditions in subsequent columns in order to allow for direct comparison of kinematic changes across experimental condition (Figure 3).

V	W	X
WK_Trunk_I_E_deg_Movement_Offset_deg	RW_Trunk_I_E_deg_Movement_Offset_deg	GW_Trunk_I_E_deg_Movement_Offset_deg
3.92	4.91	3.04
0.13	-0.66	1.95
3.82	3.89	4.59
1.21	-0.4	-0.61
-2.37	-3.79	-3.39
14.56	4.17	4.18

Figure 3. Columns V-X depict the movement offset (in degrees) for the internal/external rotation of the trunk segment during each of the three walking trials (WK, RW and GW).

The following sections will provide a detailed description of the annotation schema established for the joint articulation parameters and 3D kinematic signatures.

8.3.2. Annotation of Joint Articulations

The kinematic skeleton model utilized for the Year 3 data collection defines 14 anatomical segments. The motions of the segments, either relative to a proximal segment or to the global coordinate system (i.e. room), allowed for the definition of 14 joint movement profiles, along with one global movement profile (pelvis in global). The 3D joint kinematic metrics were calculated by employing an Euler decomposition sequence with a priority of joint flexion/extension (F/E), followed by joint abduction/adduction (Ab/Ad) about an intermediate axis, and finally internal/external (I/E) rotation about the long axis of the distal segment. The joint articulations included in the 3D kinematic analyses, along with brief descriptions of the involved body segments are provided below:

1. Trunk – represents movement of the torso relative to the pelvis
2. Pelvis – represents movement of the pelvis in the global coordinate system
3. Hip – represents movement of the thigh segment relative to the pelvis
4. Knee – represents movement of the lower leg relative to the thigh segment
5. Ankle – represents movement of the foot relative to the lower leg
6. Shoulder – represents movement of the upper arm relative to the torso
7. Elbow – represents movement of the forearm relative to the upper arm
8. Wrist – represents movement of the hand relative to the forearm
9. Head – represents movement of the head relative to the torso

Note: Joint articulation metrics are reported for both the right and left sides of the body for the hip, knee, ankle, shoulder, elbow and wrist.

8.3.3. 3D Kinematic Signature Definitions

The data collection method employed during the Year 3 activities involved the placement and tracking of retro-reflective markers on the body for the 3D kinematic assessment of skeletal motion across the three experimental walking conditions. It was hypothesized in the original proposal that, as facial movements change involuntarily in response to emotional stimuli such as deception, so might whole-body kinematics be altered by the introduction of an emotional stimulus involving deception (i.e. the concealment of a contraband item). For the kinematic assessment, we identified four joint angle waveform signatures that describe the overall functional performance of each body articulation as participants approach the security checkpoint (Figure 4). The following list provides the 3D kinematic variable abbreviations along with a description of each metric:

max angle (Max) – the largest joint angle within a gait cycle
min angle (Min) – the smallest joint angle within a gait cycle
range of motion (ROM) – the max angle minus the min angle
movement offset (Offset) – the mean of joint rotation angles throughout a gait cycle

The four metrics described above provide an indication of mean body pose during gait, along with information regarding the joint movement extremes and range. Unlike the spectral signatures, which were analyzed using the raw motion capture files, the 3D kinematic data were filtered using a low-pass, 4^{th} order Butterworth filter with a cutoff frequency of 6Hz prior to analysis. This smoothing process does not compromise the metrics to be obtained from the traditional gait analysis as the purpose of these metrics was to observe differences in movement technique not associated with movement velocity or frequencies.

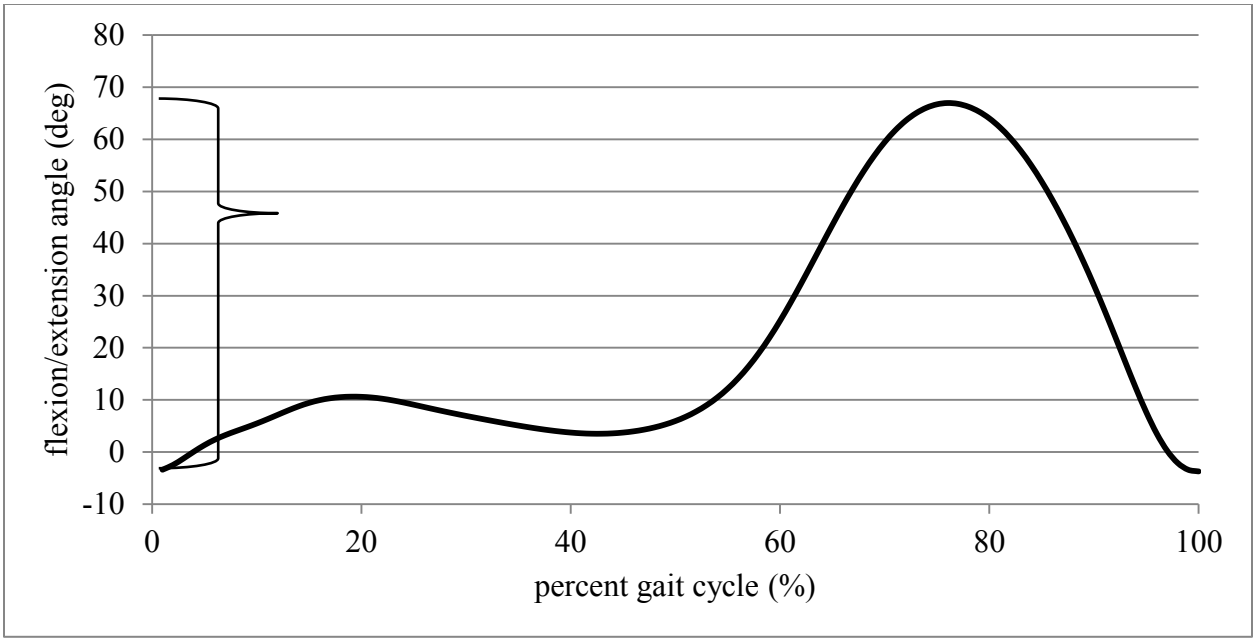

Figure 4. Representative knee flexion/extension angle profile with a depiction of the four kinematic signatures (movement offset, range of motion, max angle, min angle).

8.3.4. Temporal/Spatial Signatures Definitions

Along with joint kinematic metrics, gait is often described using basic temporal/spatial measures. Temporal/spatial descriptions of gait provide a more globalized performance definition and are generally influenced by many, if not all, of the individual joint parameters. The following temporal/spatial metrics are included in the kinematic variables spreadsheet in columns H-S:

cadence (step/min) – frequency of steps per minute
step length (cm) – linear distance between alternate heels on subsequent steps
AVG velocity (cm/min) – mean overground velocity during a gait cycle
step width (mm) – mean lateral distance between foot centers within a gait cycle

8.3.5. Variable Labeling in the Kinematic Results Spreadsheet

The first seven columns of the kinematic results spreadsheet provide the basic demographic and experimental condition data associated with each participant (as described in Section 8.2.5 above). Columns H-S of the kinematic results spreadsheet include the temporal/spatial results as described above, and the remaining metrics reported in the kinematic results spreadsheet have been labeled according to walking trial type, joint articulation, joint plane movement and kinematic metric, respectively. For example, column V in Figure 3 depicts a variable labeled "WK_Trunk_I_E_deg_Movement_Offset_deg". This signifies that the variables in this column represent the movement offset variable for the internal/external rotation movement of the trunk segment during the WK trials for all participants. The abbreviation 'deg' in each variable label merely denotes that the metric is represented in degrees. Finally, the kinematic metrics in the spreadsheet have been arranged to facilitate the direct comparison of like metrics associated with like segments across the three walking conditions.

8.4 Two-Dimensional Full-Motion Video for Facial Movement

The FMV data were collected using a Sony MiniDV Handycam® Camcorder, Model # DCR-HC38. All camera footage were saved to MiniDV tape and then transferred to a PC for processing. Once the files were transferred to a PC, the data were cut to include only the moments in a trial from the guard's instruction to approach the checkpoint to the guard's instruction to proceed through the checkpoint. Because the 2D FMV camera was only in place during the checkpoint trials, only two video data files were captured for each participant (one for each of the RW and GW trials). Figure 5 provides a screen capture depiction of the video camera perspective from behind the checkpoint.

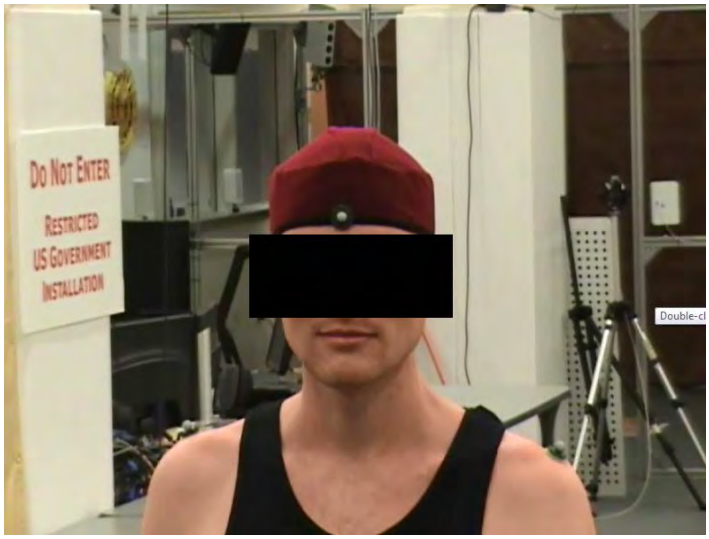

Figure 5. 2D video perspective for the RW and GW trials
The camera was positioned behind the checkpoint and aimed over the shoulder of the checkpoint guard.

9. Results

9.1 Spectral Analyses Results

9.1.1. Statistical Analyses Overview

The spectral motion analysis signatures were initially grouped to be analyzed using a 2 (condition; liar and non-liar) x 3 (walking trial; WK, RW, GW) repeated measures (RM) ANOVA. Specifically, each body segment was analyzed using a within-subject difference to identify any main effects across the three walking trial types (i.e., WK, RW, and GW) on sprectral metrics (i.e., Fp, Fmed, F95, Fratio). Where significant main effects were identified for walking trials, univariate post-hoc measures (Fisher's LSD) were used to determine which relationship(s) exhibited a significant difference. Between-subjects differences were also assessed to identify any significant difference in spectral metrics between conditions (i.e., liars and non-liars).

9.1.2. Repeated Measures ANOVA Results Tables

Below are the significant between-subjects and walking trial (WK, RW, GW) by condition (liar vs. non-liar) interactions observed from the spectral data.

LEFT FOREARM

While not significant, an interaction effect of trial x condition approached significance for Left Forearm Fmed (Table 2; $F_{2, 60.0} = 2.83$, $p = 0.06$, $\eta_p^2 = 0.08$; N-$\beta = 0.53$). No significant between-subjects effect was observed.

Table 2. Interaction Effect of Trial x Condition on Left Forearm Fmed

Trial	Liar Mean ± SD	Non-Liar Mean ± SD	P-value
WK	0.974 ± 0.09	0.977 ± 0.11	0.92
RW	0.995 ± 0.09	0.926 ± 0.10	0.05
GW	0.991 ± 0.08	0.980 ± 0.10	0.76

LEFT HAND
A repeated measures ANOVA revealed no significant trial x condition interaction effect or significant between-subjects differences.

LEFT SHANK
A repeated measures ANOVA revealed no significant trial x condition interaction effect or significant between-subjects differences.

LEFT THIGH
A repeated measures ANOVA revealed no significant trial x condition interaction effect or significant between-subjects differences.

LEFT UPPER ARM
A repeated measures ANOVA revealed no significant trial x condition interaction effect or significant between-subjects differences.

LEFT FOOT
A repeated measures ANOVA revealed no significant trial x condition interaction effect or significant between-subjects differences.

RIGHT FOOT
A repeated measures ANOVA revealed no significant trial x condition interaction effect or significant between-subjects differences.

RIGHT FOREARM

A repeated measures ANOVA revealed a significant interaction effect for trial x condition for Right Forearm Fratio (Table 3; $F_{1.4, 44.0} = 4.13$, $p = 0.03$, $\eta_p^2 = 0.12$; N-$\beta = 0.61$). No significant between-subjects effect was found.

Table 3. Interaction Effect of Trial x Condition on Right Forearm Fratio

Trial	Liar Mean ± SD	Non-Liar Mean ± SD	P-value
WK	0.33 ± 0.11	0.346 ± 0.112	0.73
RW	0.292 ± 0.12	0.384 ± 0.22	0.17
GW	0.349 ± 0.10	0.299 ± 0.13	0.25

RIGHT HAND

A repeated measures ANOVA revealed no significant interaction effect for any Right Hand metrics. However, a significant difference ($F_{1, 30} = 6.4$, $p = 0.01$, $\eta_p^2 = 0.17$; N-$\beta = 0.69$) in F95 was found between non-liar (4.985 ± 1.22) and liar groups (6.114 ± 1.94) for the Right Hand.

RIGHT SHANK

A repeated measures ANOVA revealed no significant trial x condition interaction effect or significant between-subjects differences.

RIGHT THIGH

A repeated measures ANOVA revealed no significant trial x condition interaction effect or significant between-subjects differences.

RIGHT UPPER ARM

A repeated measures ANOVA revealed a significant interaction effect for trial by condition for Right Upper Arm Fp (Table 4; $F_{1.4, 42.1} = 3.2$, $p = 0.067$, $\eta_p^2 = 0.096$; N-$\beta = 0.489$), Fmed (Table 5; $F_{2, 60} = 3.16$, $p = 0.04$, $\eta_p^2 = 0.09$; N-$\beta = 0.58$), and F95 (Table 6; $F_{2, 60} = 3.5$, $p = 0.03$, $\eta_p^2 = 0.10$; N-$\beta = 0.63$). No between-subjects main effect was found.

Table 4. Interaction Effect of Trial x Condition on Right Upper Arm Fp

Trial	Liar Mean ± SD	Non-Liar Mean ± SD	P-value
WK	0.954 ± 0.08	0.905 ± 0.06	0.07
RW	0.951 ± 0.10	0.865 ± 0.20	0.14
GW	0.959 ± 0.08	0.995 ± 0.07	0.21

Table 5. Interaction Effect of Trial x Condition on Right Upper Arm Fmed

Trial	Liar Mean ± SD	Non-Liar Mean ± SD	P-value
WK	1.14 ± 0.20	1.12 ± 0.22	0.84
RW	1.21 ± 0.27	1.07 ± 0.25	0.12
GW	1.18 ± 0.23	1.19 ± 0.20	0.95

Table 6. Interaction Effect of Trial x Condition on Right Upper Arm F95

Trial	Liar Mean ± SD	Non-Liar Mean ± SD	P-value
WK	10.3 ± 3.9	9.3 ± 2.9	0.43
RW	12.5 ± 8.2	8.0 ± 0.7	0.04
GW	12.7 ± 7.5	9.0 ± 2.2	0.06

9.2 3D Kinematic Analyses Results

9.2.1. Statistical Analyses Overview

The 3D kinematic data were initially grouped to be analyzed using a 2 (condition; liar and non-liar) x 3 (walking trial; WK, RW, GW) repeated measures (RM) ANOVA to identify differences between condition and interactions among condition and trial. Between-subjects differences were assessed to identify any significant differences in kinematic measures between conditions (i.e., liars and non-liars). When significant differences were found between group grand means, independent t-tests were performed between groups to identify which walking trials resulted in significant differences.

9.2.2. Repeated Measures ANOVA Results Tables

Below are the significant between-subjects and walking trial (WK, RW, GW) by condition (liar vs. non-liar) interactions found from the kinematic data.

<u>ANKLE</u>
A repeated measures ANOVA revealed a significant interaction effect for Ankle I/E_ROM (Table 7; $F_{2, 124} = 3.3$, $p = 0.03$, $\eta_p^2 = 0.05$; N-β = 0.62), F/E_ROM (Table 8; $F_{1.6, 103.6} = 4.2$, $p = 0.02$, $\eta_p^2 = 0.06$; N-β = 0.68), and F/E_Min (Table 9; $F_{2, 124} = 3.7$, $p = 0.02$, $\eta_p^2 = 0.05$; N-β = 0.67). No significant between-subjects main effect was found.

Distribution A: Approved for Public Release 88ABW-2016-0244; 25 January 2016

Table 7. Interaction Effect of Trial x Condition on Ankle I/E_ROM

Trial	Liar Mean ± SD	Non-Liar Mean ± SD	P-value
WK	15.8 ± 3.3	16.53 ± 4.3	0.50
RW	16.0 ± 3.6	15.75 ± 4.2	0.78
GW	16.0 ± 3.3	16.62 ± 4.6	0.58

Table 8. Interaction Effect of Trial x Condition on Ankle F/E_ROM

Trial	Liar Mean ± SD	Non-Liar Mean ± SD	P-value
WK	32.1 ± 3.6	32.2 ± 4.2	0.95
RW	32.0 ± 3.9	31.4 ± 4.6	0.58
GW	31.9 ± 4.2	32.5 ± 4.2	0.54

Table 9. Interaction Effect of Trial x Condition on Ankle F/E_Min

Trial	Liar Mean ± SD	Non-Liar Mean ± SD	P-value
WK	-7.3 ± 5.5	-6.4 ± 4.4	0.49
RW	-7.8 ± 6.0	-6.2 ± 5.2	0.26
GW	-7.35 ± 6.1	-7.0 ± 4.4	0.80

ELBOW

A repeated measures ANOVA revealed a significant interaction effect for Elbow F/E_Offset (Table 10; $F_{2, 124} = 5.3$, $p = 0.006$, $\eta_p^2 = 0.08$; N-$\beta = 0.83$). No significant between-subjects main effect was found.

Table 10. Interaction Effect of Trial x Condition on Elbow F/E_Offset

Trial	Liar Mean ± SD	Non-Liar Mean ± SD	P-value
WK	23.9 ± 10.2	23.4 ± 10.5	0.83
RW	24.5 ± 10.7	23.7 ± 10.8	0.76
GW	24.2 ± 10.0	24.8 ± 10.8	0.79

HIP

A repeated measures ANOVA revealed no significant main effect between subjects, however, a significant interaction effect for the following variables was observed:

Hip I/E_ROM- (Table 11; $F_{1.8, 113.0} = 5.4$, $p = 0.003$, $\eta_p^2 = 0.09$; N-β = 0.87)
Hip I/E_Min- (Table 12; $F_{2, 124} = 4.7$, $p = 0.01$, $\eta_p^2 = 0.07$; N-β = 0.77)
Hip Ab/Ad_ROM- (Table 13; $F_{2, 124} = 6.1$, $p = 0.003$, $\eta_p^2 = 0.09$; N-β = 0.88)
Hip Ab/Ad_Max- (Table 14; $F_{2, 124} = 3.5$, $p = 0.03$, $\eta_p^2 = 0.05$; N-β = 0.64)
Hip F/E_Offset- (Table 15; $F_{1.6, 103.4} = 4.3$, $p < 0.01$, $\eta_p^2 = 0.12$; N-β = 0.87)
Hip F/E_ROM- (Table 16; $F_{2, 124} = 3.9$, $p = 0.02$, $\eta_p^2 = 0.06$; N-β = 0.70)
Hip F/E_Max- (Table 17; $F_{1.7, 105.6} = 3.9$, $p = 0.002$, $\eta_p^2 = 0.09$; N-β = 0.87)
Hip F/E_Min- (Table 18; $F_{2, 124} = 6.2$, $p = 0.002$, $\eta_p^2 = 0.09$; N-β = 0.88)

Table 11. Interaction Effect of Trial x Condition on Hip I/E_ROM

Trial	Liar Mean ± SD	Non-Liar Mean ± SD	P-value
WK	18.6 ± 2.7	19.6 ± 4.19	0.27
RW	19.1 ± 2.9	19.3 ± 4.5	0.84
GW	18.8 ± 3.0	20.1 ± 4.3	0.18

Table 12. Interaction Effect of Trial x Condition on Hip I/E_Min

Trial	Liar Mean ± SD	Non-Liar Mean ± SD	P-value
WK	-14.8 ± 7.5	-14.6 ± 8.2	0.93
RW	-15.2 ± 7.3	-14.8 ± 8.1	0.83
GW	-15.1 ± 7.4	-15.6 ± 8.3	0.80

Table 13. Interaction Effect of Trial x Condition on Hip Ab/Ad_ROM

Trial	Liar Mean ± SD	Non-Liar Mean ± SD	P-value
WK	14.7 ± 3.2	15.1 ± 4.1	0.69
RW	15.3 ± 3.3	15.0 ± 4.1	0.77
GW	15.3 ± 3.0	15.9 ± 3.9	0.51

Table 14. Interaction Effect of Trial x Condition on Hip Ab/Ad_Max

Trial	Liar Mean ± SD	Non-Liar Mean ± SD	P-value
WK	7.6 ± 4.2	7.6 ± 4.5	0.97
RW	7.7 ± 4.7	7.3 ± 4.6	0.67
GW	7.7 ± 4.5	7.8 ± 4.8	0.99

Table 15. Interaction Effect of Trial x Condition on Hip F/E_Offset

Trial	Liar Mean ± SD	Non-Liar Mean ± SD	P-value
WK	16.8 ± 7.9	15.53 ± 7.5	0.51
RW	16.9 ± 7.4	15.62 ± 7.4	0.50
GW	15.7 ± 7.2	15.30 ± 7.0	0.82

Table 16. Interaction Effect of Trial x Condition on Hip F/E_ROM

Trial	Liar Mean ± SD	Non-Liar Mean ± SD	P-value
WK	43.6 ± 5.0	43.2 ± 4.8	0.76
RW	44.7 ± 5.3	42.6 ± 5.1	0.13
GW	44.7 ± 4.7	44.8 ± 4.6	0.93

Table 17. Interaction Effect of Trial x Condition on Hip F/E_Max

Trial	Liar Mean ± SD	Non-Liar Mean ± SD	P-value
WK	36.1 ± 8.7	34.5 ± 7.5	0.44
RW	36.5 ± 8.3	34.7 ± 7.7	0.37
GW	35.5 ± 7.9	34.9 ± 7.2	0.74

Table 18. Interaction Effect of Trial x Condition on Hip F/E_Min

Trial	Liar Mean ± SD	Non-Liar Mean ± SD	P-value
WK	-7.5 ± 7.5	-8.7 ± 7.9	0.54
RW	-8.2 ± 7.1	-7.9 ± 8.0	0.91
GW	-9.17 ± 7.0	-9.9 ± 6.9	0.68

KNEE

A repeated measures ANOVA revealed an interaction effect of trial x condition for Knee I/E_ROM (Table 19; $F_{2, 124} = 5.8$, $p = 0.04$, $\eta_p^2 = 0.08$; N-β = 0.86), I/E_Max (Table 20; $F_{2, 124} = 5.7$, $p = 0.04$, $\eta_p^2 = 0.08$; N-β = 0.85), and F/E_ROM (Table 21; $F_{2, 124} = 3.9$, $p = 0.02$, $\eta_p^2 = 0.06$; N-β = 0.70).

Table 19. Interaction Effect of Trial x Condition on Knee I/E_ROM

Trial	Liar Mean ± SD	Non-Liar Mean ± SD	P-value
WK	23.8 ± 4.9	28.2 ± 5.3	<0.01
RW	24.4 ± 4.9	27.6 ± 5.2	0.01
GW	23.9 ± 5.1	28.8 ± 5.1	<0.01

Table 20. Interaction Effect of Trial x Condition on Knee I/E_Max

Trial	Liar Mean ± SD	Non-Liar Mean ± SD	P-value
WK	7.2 ± 9.0	9.9 ± 8.0	0.22
RW	7.7 ± 8.6	9.6 ± 8.6	0.38
GW	7.6 ± 8.5	10.6 ± 8.8	0.16

Table 21. Interaction Effect of Trial x Condition on Knee F/E_ROM

Trial	Liar Mean ± SD	Non-Liar Mean ± SD	P-value
WK	68.8 ± 3.6	71.7 ± 4.0	<0.01
RW	69.4 ± 4.1	71.0 ± 4.4	0.15
GW	70.2 ± 4.2	72.4 ± 4.4	0.04

Analyses also revealed a significant main effect of condition on Knee I/E_ROM where the non-liar group exhibited significantly greater I/E_ROM than the liar group (28.1 ± 5.2 vs. 24.0 ± 4.9; $F_{1, 62} = 10.9$, $p = 0.002$, $\eta_p^2 = 0.15$; N-β = 0.90). Non-liars also produced significantly greater Knee F/E_ROM (71.7 ± 4.29) than the liar group (69.4 ± 3.9; $F_{1, 62} = 4.7$, $p = 0.03$, $\eta_p^2 = 0.17$; N-β = 0.57) as well as significantly higher Knee Ab/Ad_ROM- ($F_{1, 62} = 9.1$, $p = 0.004$, $\eta_p^2 = 0.12$; N-β = 0.84) in the non-liar group (17.2 ± 4.3) than liars (14.4 ± 3.2).

PELVIS

A repeated measures ANOVA revealed no significant main effect on subject, however, a significant interaction effect of trial x condition was observed for the following variables:

Pelvis I/E_Offset- (Table 22; $F_{1.7, 110.7} = 4.2$, $p = 0.02$, $\eta_p^2 = 0.06$; N-β = 0.69)
Pelvis I/E_Max- (Table 23; $F_{1.7, 110.7} = 6.6$, $p = 0.004$, $\eta_p^2 = 0.08$; N-β = 0.84)
Pelvis Ab/Ad_ROM- (Table 24; $F_{2, 124} = 6.4$, $p = 0.002$, $\eta_p^2 = 0.09$; N-β = 0.89)
Pelvis Ab/Ad_Min- (Table 25; $F_{1.7, 111.3} = 4.2$, $p = 0.02$, $\eta_p^2 = 0.06$; N-β = 0.70)
Pelvis F/E_ROM- (Table 26; $F_{2, 124} = 3.7$, $p = 0.02$, $\eta_p^2 = 0.05$; N-β = 0.68)

Table 22. Interaction Effect of Trial x Condition on Pelvis I/E_Offset

Trial	Liar Mean ± SD	Non-Liar Mean ± SD	P-value
WK	-8.8 ± 6.3	-7.2 ± 6.0	0.29
RW	-9.0 ± 5.7	-7.4 ± 6.2	0.29
GW	-7.7 ± 5.6	-6.8 ± 5.9	0.53

Table 23. Interaction Effect of Trial x Condition on Pelvis I/E_Max

Trial	Liar Mean ± SD	Non-Liar Mean ± SD	P-value
WK	-6.8 ± 6.3	-5.1 ± 6.1	0.27
RW	-7.1 ± 5.7	-5.4 ± 6.3	0.27
GW	-5.4 ± 5.5	-4.6 ± 6.1	0.55

Table 24. Interaction Effect of Trial x Condition on Pelvis Ab/Ad_ROM

Trial	Liar Mean ± SD	Non-Liar Mean ± SD	P-value
WK	8.4 ± 2.1	9.0 ± 3.1	0.37
RW	8.8 ± 2.4	8.9 ± 3.1	0.50
GW	8.9 ± 2.3	9.6 ± 2.9	0.30

Table 25. Interaction Effect of Trial x Condition on Pelvis Ab/Ad_Min

Trial	Liar Mean ± SD	Non-Liar Mean ± SD	P-value
WK	-4.7 ± 2.0	-5.0 ± 2.9	0.67
RW	-5.0 ± 2.2	-4.9 ± 2.9	0.98
GW	-4.8 ± 2.2	-5.3 ± 3.2	0.46

Table 26. Interaction Effect of Trial x Condition on Pelvis F/E_ROM

Trial	Liar Mean ± SD	Non-Liar Mean ± SD	P-value
WK	14.7 ± 4.7	17.4 ± 4.5	0.02
RW	16.1 ± 4.6	17.4 ± 4.2	0.27
GW	16.0 ± 5.0	18.0 ± 5.1	0.13

SHOULDER

A repeated measures ANOVA revealed a significant interaction effect for Shoulder I/E_Offset (Table 27; $F_{2, 124} = 3.1$, $p = 0.04$, $\eta_p^2 = 0.04$; N-$\beta = 0.59$) and Ab/Ad_Offset (Table 28; $F_{2, 124} = 3.9$, $p = 0.02$, $\eta_p^2 = 0.06$; N-$\beta = 0.20$).

Table 27. Interaction Effect of Trial x Condition on Shoulder I/E_Offset

Trial	Liar Mean ± SD	Non-Liar Mean ± SD	P-value
WK	21.2 ± 24.7	10.4 ± 32.4	0.14
RW	20.5 ± 25.4	9.9 ± 32.9	0.15
GW	19.1 ± 25.5	9.7 ± 32.9	0.21

Table 28. Interaction Effect of Trial x Condition on Shoulder Ab/Ad_Offset

Trial	Liar Mean ± SD	Non-Liar Mean ± SD	P-value
WK	7.9 ± 4.1	7.8 ± 4.0	0.94
RW	8.1 ± 4.3	8.2 ± 4.2	0.91
GW	8.1 ± 3.9	8.6 ± 4.3	0.62

TRUNK

A repeated measures ANOVA revealed a significant interaction effect for the following variables:

Trunk I/E_ROM- (Table 29; $F_{1.7,\ 106.6} = 8.3$, $p = 0.001$, $\eta_p^2 = 0.11$; N-β = 0.93)
Trunk I/E_Max- (Table 30; $F_{1.6,\ 101.6} = 7.3$, $p = 0.002$, $\eta_p^2 = 0.10$; N-β = 0.89)
Trunk Ab/Ad_ROM- (Table 31; $F_{2,\ 124} = 6.9$, $p = 0.001$, $\eta_p^2 = 0.10$; N-β = 0.91)
Trunk Ab/Ad_Max- (Table 32; $F_{1.7,\ 109.7} = 4.1$, $p = 0.02$, $\eta_p^2 = 0.06$; N-β = 0.68)

Table 29. Interaction Effect of Trial x Condition on Trunk I/E_ROM

Trial	Liar Mean ± SD	Non-Liar Mean ± SD	P-value
WK	18.5 ± 5.8	23.2 ± 4.5	0.001
RW	20.1 ± 5.9	22.5 ± 5.2	0.09
GW	20.1 ± 5.8	24.0 ± 4.5	0.004

Table 30. Interaction Effect of Trial x Condition on Trunk I/E_Max

Trial	Liar Mean ± SD	Non-Liar Mean ± SD	P-value
WK	10.1 ± 3.7	10.5 ± 3.3	0.72
RW	11.4 ± 4.2	10.2 ± 3.6	0.21
GW	11.0 ± 4.4	10.8 ± 3.2	0.88

Table 31. Interaction Effect of Trial x Condition on Trunk Ab/Ad_ROM

Trial	Liar Mean ± SD	Non-Liar Mean ± SD	P-value
WK	9.7 ± 2.2	11.0 ± 2.9	0.04
RW	10.5 ± 2.9	11.1 ± 3.1	0.38
GW	10.3 ± 2.7	12.0 ± 2.9	0.02

Table 32. Interaction Effect of Trial x Condition on Trunk Ab/Ad_Max

Trial	Liar Mean ± SD	Non-Liar Mean ± SD	P-value
WK	5.4 ± 2.0	5.6 ± 1.9	0.61
RW	5.9 ± 2.3	5.8 ± 2.0	0.91
GW	5.4 ± 2.0	6.0 ± 2.1	0.28

Analyses also revealed significant differences between subjects for the following variables:

Trunk I/E_Offset-($F_{1, 62} = 14.4$, $p < 0.001$, $\eta_p^2 = 0.18$; N-β = 0.96). Liars significantly higher than non-liars (1.1 ± 2.8 vs. -1.2 ± 1.9).
Trunk I/E_ROM- ($F_{1, 62} = 8.0$, $p = 0.006$, $\eta_p^2 = 0.11$; N-β = 0.79). Non-liars significantly higher than liars (23.2 ± 4.7 vs. 19.6 ± 5.8).
Trunk I/E_Min- ($F_{1, 62} = 20.6$, $p < 0.001$, $\eta_p^2 = 0.25$; N-β = 0.99). Liars significantly greater than non-liars (-8.7 ± 4.1 vs. -12.7 ± 3.0).
Trunk F/E_Offset- ($F_{1, 62} = 5.1$, $p = 0.02$, $\eta_p^2 = 0.07$; N-β = 0.61). Liars significantly less than non-liars (-6.7 ± 6.2 vs. -2.5 ± 6.6).
Trunk F/E_Max-($F_{1, 62} = 5.1$, $p = 0.02$, $\eta_p^2 = 0.07$; N-β = 0.60). Liars significantly less than non-liars (-3.7 ± 6.1 vs. -0.05 ± 6.6).
Trunk F/E_Min- ($F_{1, 62} = 4.4$, $p = 0.04$, $\eta_p^2 = 0.06$; N-β = 0.54). Liars significantly less than non-liars (-9.1 ± 6.2 vs. -5.7 ± 6.8).

WRIST

A repeated measures ANOVA revealed a significant interaction effect for Wrist F/E_ROM (Table 33; $F_{2, 124} = 3.4$, $p = 0.03$, $\eta_p^2 = 0.05$; N-β = 0.63) and F/E_Max (Table 34; $F_{2, 124} = 3.9$, $p = 0.02$, $\eta_p^2 = 0.05$; N-β = 0.69).

Distribution A: Approved for Public Release 88ABW-2016-0244; 25 January 2016

Table 33. Interaction Effect of Trial x Condition on Wrist F/E_ROM

Trial	Liar Mean ± SD	Non-Liar Mean ± SD	P-value
WK	10.2 ± 4.4	11.5 ± 5.9	0.31
RW	11.4 ± 5.7	10.9 ± 7.2	0.79
GW	11.4 ± 5.7	13.1 ± 7.9	0.33

Table 34. Interaction Effect of Trial x Condition on Wrist F/E_Max

Trial	Liar Mean ± SD	Non-Liar Mean ± SD	P-value
WK	2.6 ± 9.6	-2.3 ± 15.1	0.11
RW	3.9 ±9.3	-2.6 ± 14.8	0.03
GW	3.7 ± 9.7	-1.0 ± 15.4	0.14

9.3 Logistic Regression Modeling for Deception Prediction

9.3.1. Statistical Analyses Overview

Continuous data were subjected to binomial logistic multiple regression analyses utilizing a backwards step-wise method based upon likelihood ratios. The logistic regression approach was used to yield a series of models to predict the probability of an individual being deceptive based on changes in measured kinematic and spectral metrics. The use of a logistic regression approach to yield prediction equations is preferable to OLS linear regression analyses as it deviates from traditional statistical assumptions. Specifically, logistic regression does not assume a linear relationship between dependent and independent variables, the dependent variable does not need to be normally distributed, the independent variables need not be interval and the independents need not be unbound. All data were analyzed utilizing the Statistical Package for Social Sciences (SPSS, v.19.0, Chicago, IL).

The dependent (outcome) variable in this model was binary. The binary nature of the variable was a simple 'liar' or 'non-liar' with respect to the condition in which the data were collected. A 'liar' was coded as '1', was the value being predicted and refers to a condition in which the participant was being deceptive. Similarly, a 'non-liar' was coded as '0' and was the control condition from which the probabilities were based.

9.3.2. Prediction Probability

The output reports from SPSS detail the stepwise procedures for each series of analyses using Wald statistic values for logistic regression. This procedure yielded multiple significant ($p < 0.05$) models, with each step providing improvements that were considered significant for each condition. Accordingly, the R^2 values associated with the models were adequate and are

provided in the model summary tables (use Nagelkerke's). Importantly, R^2 values in logistic regression are not to be viewed similar to R^2 values from OLS regression measures. While critically important in OLS, the R^2 is of less value (albeit still useful) in terms of the utility of the equation.

Also, the results from the Hosmer and Lemeshow tests demonstrate acceptable goodness of fit for the equation and the data. Each model's goodness of fit is addressed singularly below with each condition. Additionally, the contingency table is provided and addressed, which divides the data into deciles and tests predictive outcomes against anticipated outcomes.

Critical to predictive model selection is the classification model. These tables demonstrate the predictive ability of the model using the derived constant as well as the predictor variables that have been selected using the likelihood ratio to improve model fit. These data, paired with Hosmer and Lemeshow goodness of fit were requisite for selecting the most parsimonious probability prediction models.

The tables presented for each condition contain the variables that were employed in each stepwise equation modeled, including the constant. Each step adds a predictor variable based upon its partial correlation strength to add to the predictive ability of the model. The 'B' column is the coefficient and each variable should be significant with the standard error is shown in the S.E. column. Also shown is the EXP(B), which is the corresponding odds ratio for that particular variable relative to the control condition as well as the 95% confidence interval for the odds ratio.

9.3.2. Logistic Regression Model

The stepwise logistic regression analysis provided 10 significant models. We have selected, based upon parsimony of the variables included relative to prediction precision, model 10 from the analysis. Below is selected output from the complete analysis.

As shown below in Table 35, the model was significant at $p < 0.001$. Table 36 demonstrates the goodness of fit of the step 10 model. In general, the greater the degree of significance, in this case $p = 0.588$, the better the model fit. Also, the Nagelkerke R^2, while not as important in indicating goodness of fit, does demonstrate adequate variance explained with an $R^2 = 0.627$.

Table 35. Omnibus test of model coefficients and model significance (N=32)

		Chi-square	df	Sig.
Step 10[a]	Step	-1.415	1	.234
	Block	20.331	3	.000
	Model	20.331	3	.000

Distribution A: Approved for Public Release 88ABW-2016-0244; 25 January 2016

Table 36. Hosmer and Lemeshow Test results of model goodness of fit (N = 32)

Step	Chi-square	df	Sig.
1	.000	7	1.000
2	.000	7	1.000
3	.000	7	1.000
4	.000	7	1.000
5	.000	6	1.000
6	3.282	8	.915
7	3.692	8	.884
8	6.411	8	.601
9	13.270	8	.103
10	6.530	8	.588

Table 37. Logistic regression model summary

Step	-2 Log likelihood	Cox & Snell R Square	Nagelkerke R Square
1	.000[a]	.750	1.000
2	.000[a]	.750	1.000
3	.000[a]	.750	1.000
4	.000[a]	.750	1.000
5	.000[a]	.750	1.000
6	19.475[b]	.541	.721
7	19.553[b]	.539	.719
8	21.635[b]	.508	.678
9	22.615[b]	.493	.658
10	24.030[c]	.470	.627

Table 38 shows the resulting contingency table that presents the classification of predicted group based upon the probability equation. As shown, each decile produced an adequate observation to expectancy ratio.

Table 38. Contingency table for Hosmer and Lemeshow tests showing decile placements from the probability prediction equations (N=32)

		Liar = Non-Liar		Liar = Liar		
		Observed	Expected	Observed	Expected	Total
Step 10	1	3	2.936	0	.064	3
	2	3	2.804	0	.196	3
	3	2	2.674	1	.326	3
	4	2	2.301	1	.699	3
	5	3	1.950	0	1.050	3
	6	1	1.452	2	1.548	3
	7	2	.990	1	2.010	3
	8	0	.663	3	2.337	3
	9	0	.172	3	2.828	3
	10	0	.059	5	4.941	5

Below is the classification table (Table 39) demonstrating the aggregate predictive accuracy of the model. In total, the model demonstrates 81.3% predictive accuracy, with identical accuracy of prediction to the non-liar condition versus assignment to the liar group.

Table 39. Classification table resulting from the probability prediction equations (N=32)

			Predicted		
			Liar		Percentage
	Observed		Non-Liar	Liar	Correct
Step 10	Liar	Non-Liar	13	3	81.3
		Liar	3	13	81.3
	Overall Percentage				81.3

Finally, Table 40 reveals the constant (intercept) and coefficients for building the prediction model, standard error, level of significance and the respective odds ratio and the 95% level of confidence of each coefficient.

Table 40. Model construction table with the variables and constant included in the probability prediction equations (N = 32)

		B	S.E.	Wald	df	Sig.	Exp(B)	95% C.I.for EXP(B)	
								Lower	Upper
Step 10[a]	GW_Trunk_I_E_deg_Movement_Offset_deg	.621	.245	6.405	1	.011	1.861	1.150	3.012
	GW_Trunk_I_E_deg_Range_of_Motion_deg	-.304	.149	4.136	1	.042	.738	.550	.989
	GW_Knee_F_E_deg_Range_of_Motion_deg	-.342	.152	5.097	1	.024	.710	.528	.956
	Constant	31.261	12.901	5.872	1	.015	37720305286608.850		

Final Probability Prediction Equation:

$P_{(Liar)}=1/1+e^{-(31.26+(0.621*\text{Trunk\_I/E\_Movement Offset})-(0.304*\text{Trunk\_I/E\_ROM})-(0.342*\text{Knee\_F/E\_ROM})}$

In summary, the results from the stepwise logistic regression analyses yielded a significant probability prediction model to identify liars and non-liars. The model demonstrates adequate acceptability and utility. There are a number of limitations that are important to acknowledge with the degree of prediction accuracy of these models. Specifically, these models, when/if implemented into a large sample or population of individuals may not yield such robust prediction rates. That is, the degree of 'correct' prediction (from the classification tables in the description of the models) is going to be inflated because the logistic model is predicting classification based upon the data from which the equation was derived. In order to more thoroughly investigate the utility of this model to identify individuals in these conditions, a cross-validation analysis should be performed.

9.4 Year 2 vs. Year 3 Population Comparison (U.S. vs. non-U.S.)

9.4.1. Spectral MANOVA Results

A MANOVA comparison of U.S. and non-U.S. participant's spectral metrics revealed a significant main effect for population ($F_{37.51} = 17.4$; $p<0.01$; $\eta^2_p = 0.96$; N-B=1.0). However, there was no main effect for lie condition ($p = 0.07$) and there was no significant population by lie condition interaction ($p = 0.19$).

Table 41 shows where univariate post-hoc measures (Fisher's LSD) revealed significantly higher values in the U.S. population (vs. the non-U.S.) for the following body segments and spectral metrics.

Table 41. Post-hoc significance values for the U.S. vs. non-U.S. comparison of spectral metrics *(where mean values were significantly greater in the U.S. sample)*

SEGMENT	METRIC	P-VALUE
HEAD	F95	<0.01
LEFT UPPER ARM	F95	<0.01
LEFT FOREARM	F95	<0.01
	Fratio	<0.01
LEFT HAND	F95	<0.01
RIGHT UPPER ARM	F95	<0.01
RIGHT FOREARM	F95	<0.01
	Fratio	0.04
RIGHT HAND	F95	<0.01
LEFT THIGH	F95	<0.01
RIGHT THIGH	F95	<0.01
RIGHT SHANK	F95	<0.01
	Fratio	<0.01
RIGHT FOOT	F95	<0.01

Table 42 shows where univariate post-hoc measures (Fisher's LSD) revealed significantly higher values in the non-U.S. population (vs. the U.S.) for the following body segments and spectral metrics.

Table 42. Post-hoc significance values for the U.S. vs. non-U.S. comparison of spectral metrics *(where mean values were significantly greater in the non-U.S. sample)*

SEGMENT	METRIC	P-VALUE
HEAD	Fp	<0.01
	Fmed	<0.01
LEFT UPPER ARM	Fp	<0.01
LEFT FOREARM	Fp	<0.01
LEFT HAND	Fp	<0.01
RIGHT UPPER ARM	Fp	<0.01
RIGHT FOREARM	Fp	<0.01
RIGHT HAND	Fp	<0.01
LEFT SHANK	Fp	<0.01
	Fmed	<0.01
	Fratio	0.04
LEFT FOOT	Fp	<0.01
	Fmed	<0.01
RIGHT THIGH	Fp	<0.01
	Fratio	<0.01
RIGHT SHANK	Fp	<0.01
RIGHT FOOT	Fp	<0.01
	Fmed	<0.01

9.4.2. Kinematic MANOVA Results

A MANOVA comparison of U.S. and non-U.S. participant's kinematic metrics revealed a significant main effect for population ($F_{84,95} = 59.1$; $p<0.01$; $\eta^2_p = 0.98$; N-B=1.0) and for the lie condition ($F_{84,95} = 1.7$; $p<0.01$; $\eta^2_p = 0.66$; N-B=1.0). However, there was no significant population by lie condition interaction ($p = 0.058$).

Table 43 shows where univariate post-hoc measures (Fisher's LSD revealed significantly higher values in the U.S. population (vs. the non-U.S.) for the following body joints/segments and kinematic metrics.

Table 43. Post-hoc significance values for the U.S. vs. non-U.S. comparison of kinematic metrics *(where mean values were significantly greater in the U.S. sample)*

SEGMENT	METRIC	P-VALUE
TRUNK	FE_ROM	<0.01
	FE_MAX	<0.01
PELVIS	IE_OFFSET	0.03
	IE_ROM	<0.01
	IE_MAX	<0.01
	ABAD_ROM	<0.01
	ABAD_MAX	<0.01
	FE_OFFSET	0.01
	FE_MIN	<0.01
HIP	IE_OFFSET	<0.01
	IE_MAX	0.03
	IE_MIN	<0.01
KNEE	ABAD_OFFSET	<0.01
	ABAD_MIN	<0.01
ANKLE	IE_OFFSET	<0.01
	IE_MAX	<0.01
	IE_MIN	<0.01
	ABAD_ROM	<0.01
ELBOW	FE_MIN	<0.01
WRIST	IE_OFFSET	<0.01
	IE_ROM	<0.01
	IE_MAX	<0.01
	IE_MIN	<0.01
	ABAD_OFFSET	<0.01
	ABAD_ROM	<0.01
	ABAD_MAX	<0.01
	FE_OFFSET	<0.01
	FE_MAX	<0.01
	FE_MIN	<0.01

Table 44 shows where univariate post-hoc measures (Fisher's LSD) revealed significantly higher values in the non-U.S. population (vs. the U.S.) for the following body joints/segments and kinematic metrics.

Table 44. Post-hoc significance values for the U.S. vs. non-U.S. comparison of kinematic metrics *(where mean values were significantly greater in the non-U.S. sample)*

SEGMENT	METRIC	P-VALUE
TRUNK	IE_ROM	0.01
	ABAD_OFFSET	<0.01
	ABAD_MAX	<0.01
	ABAD_MIN	<0.01
PELVIS	ABAD_MIN	<0.01
	FE_ROM	0.02
HIP	IE_ROM	<0.01
	FE_OFFSET	<0.01
	FE_ROM	<0.01
	FE_MAX	<0.01
KNEE	IE_OFFSET	<0.01
	IE_ROM	<0.01
	IE_MAX	<0.01
	IE_MIN	<0.01
	ABAD_ROM	<0.01
	FE_OFFSET	<0.01
	FE_MAX	<0.01
	FE_MIN	<0.01
ANKLE	IE_ROM	<0.01
	ABAD_MIN	<0.01
	FE_OFFSET	<0.01
	FE_ROM	<0.01
	FE_MAX	<0.01
	FE_MIN	<0.01
SHOULDER	IE_OFFSET	<0.01
	IE_ROM	<0.01
	IE_MAX	<0.01
	IE_MIN	<0.01
	ABAD_ROM	<0.01
	FE_ROM	<0.01
	FE_MAX	<0.01
ELBOW	IE_OFFSET	<0.01
	IE_ROM	<0.01
	IE_MAX	<0.01
	IE_MIN	<0.01
	ABAD_OFFSET	<0.01
	ABAD_ROM	<0.01
	ABAD_MAX	<0.01
	ABAD_MIN	<0.01
	FE_ROM	<0.01
	FE_MAX	<0.01
WRIST	FE_ROM	<0.01

Table 45 shows where univariate post-hoc measures (Fisher's LSD) revealed significantly higher values in the lie condition (vs. the non-lie) for the following body segments and kinematic metrics.

Table 45. Post-hoc significance values for the lie vs. non-lie comparison of kinematic metrics *(where mean values were significantly greater in the lie sample)*

SEGMENT	METRIC	P-VALUE
TRUNK	IE_OFFSET	<0.01
	IE_MIN	<0.01
WRIST	FE_MIN	0.03

Table 46 shows where univariate post-hoc measures (Fisher's LSD) revealed significantly higher values in the non-lie condition (vs. the lie) for the following body segments and kinematic metrics.

Table 46. Post-hoc significance values for the lie vs. non-lie comparison of kinematic metrics *(where mean values were significantly greater in the non-lie sample)*

SEGMENT	METRIC	P-VALUE
TRUNK	ABAD_ROM	0.02
KNEE	IE_ROM	<0.01
	ABAD_ROM	0.02
WRIST	FE_MIN	0.03

10. Year 2 Deception Recognition Summary

The tasks associated with the Year 3 period of performance involved the collection, processing and analysis of motion capture metrics from a set of 32, non-U.S. test participants engaged in the navigation of a simulated security checkpoint under conditions of either legal small firearm concealment (non-liars) or deceptive weapon concealment (liars). The principle objective of this work was to establish the presence of a baseline set of human movement signatures capable of distinguishing between individuals carrying a contraband item either truthfully or deceptively. As all test participants completed a checkpoint approach trial involving the possession of a concealed firearm, the distinctive feature between the different experimental groups involved their intent to either declare the legal carriage of the firearm, or to attempt clandestine transport of the firearm through the checkpoint. The far-term objective of this work is to determine not only that such whole-body movement cues exist (to some degree) for detecting human deception at a distance, but also that such macro-scale human dynamic signatures present with a degree of universality, rather than being culturally derived. The current data collection and analyses build upon the products of the Year 2 work by collecting a matched data set from a group of non-U.S. test participants (whereas Year 2 involved U.S.-born participants).

As with the Year 2 data, the human movement signatures investigated during the current analyses were organized into two distinct categories: 1) spectral movement signatures, and 2) traditional 3D kinematic signatures. The principle difference between these categories is that

traditional 3D kinematic signatures require the *a priori* definition of a skeleton model for data collection and analyses. For example, before the knee joint and associated joint angles can be derived, one must first identify, and model both the thigh and lower-leg segments. Skeleton modeling for human tracking can involve extensive and time-consuming optimization in order to achieve even modest levels of skeletal tracking fidelity. In cases where traditional 2D surveillance video data are used for human tracking and modeling, a skeleton model must be applied in each frame of each video clip, potentially resulting in an optimization process that is impractical to execute in real-time. For this reason, other sensor modes have been, and are being, considered as alternatives to standard 2D video tracking. Specifically, there is interest in the application of radar-based human tracking as there is no skeletal modeling requirement. The spectral signatures described in this report, while derived from the 3D motion capture data, represent data that are based upon movement frequencies rather than spatial movement qualities. It was anticipated that, if predictive cues related to the spectral motion signatures were observed, there may be the possibility to achieve deception prediction with radar-based, or other, modalities rather than video-based modalities.

As with the findings previously reported for a U.S.-born sample, both categories of variable (spectral and kinematic) provided predictor variables for deception detection in non-U.S. participants, however, there were clearly more variables observed from the kinematics category (>20 compared to four spectral variables). In the previous U.S. sample, the single spectral metric that provided deception prediction came from the Left Shank segment. However, in the current non-U.S. sample, the four spectral metrics exhibiting differences between lie conditions were derived from upper extremity body segments (i.e. both Forearms and the Right Upper Arm). This finding was further reinforced by the observation that the respective spectral metrics were found to be significantly different between populations (Tables 41 & 42). The discrepancy in the anatomical sources of the predictive spectral metrics may suggest a cultural gait difference between the presented U.S. and non-U.S. (predominantly Indian) populations. 3D kinematic signatures from nearly every anatomical joint were found to be significantly different between liars and non-liars in the non-U.S. sample. For consistency, the predictive spectral signatures observed for the non-U.S. sample were pooled with the significant 3D kinematic signatures for final logistic regression prediction modeling.

Following the backwards step-wise method described for the Year 2 analysis, a single logistic regression model was identified. The final prediction model for the non-U.S. sample included three kinematics metrics (Trunk_I/E_ROM, Trunk_I/E_Offset, and Knee_F/E_ROM). Unlike the model derived previously for the U.S. sample, the non-U.S. prediction model did not include any of the spectral metrics. Also, the one gait metric ultimately incorporated into both prediction models was Trunk_I/E_ROM. This finding may suggest some type of universal influence of deception on the rotation of the trunk during an ECP approach scenario. Further research with a more varied sample of culturally diverse test participants would be required to confirm that hypothesis. The non-U.S. prediction model demonstrated an overall correct classification rate (CCR) of 81.3%, with a CCR of 81.3% for the prediction of both non-liars and liars (Table 39). Interestingly, while the overall CCR of the non-U.S. model was nearly 10% greater than that of the U.S. model (81.3% vs. 72.9%, respectively), both models demonstrated a CCR of approximately 80% for the prediction of non-liars, whereas the CCRs for the prediction of lairs were 81.3% and 56.8% for the non-U.S. and U.S. samples, respectively. These data seem to

suggest that, despite comparable prediction of non-deceptive contraband carriage, whole-body gait features are more useful for predicting deceptive contraband concealment in the non-U.S. population compared to individuals from the U.S. The current findings do not shed light on why these predictive differences exist, but it is possible that future research regarding social-cultural differences in deception strategies may explicate this phenomenon.

One notably intriguing difference observed between the U.S. and non-U.S. samples involved the particular between-sample differences associated with the spectral gait metrics. Specifically, Tables 41 and 42 show that the U.S. sample presented greater values for multiple F95 metrics compared to the non-U.S. samples, which presented greater values for multiple Fp metrics. This finding, that the U.S. sample tended to have larger F95 and smaller Fp metrics compared to non-U.S. participants, would seem to suggest that gait spectral content are less spread, and more centrally focused at lower movement frequencies in the non-U.S. sample. It is unclear what this finding may suggest for differences in the prediction of deception across varying cultures but again, future research into social-cultural differences may help to better interpret this difference.

The results of the current Year 3 (non-U.S.), along with the non-U.S. vs. U.S., analyses demonstrate the proof-of-concept proposed for the LRIR effort. Namely, that there is information content in whole-body human movement that may indicate deception/concealment on the part of an individual approaching a checkpoint. Further, the findings from the cross-cultural analyses support the hypothesis that predictive differences in whole-body movement may present across cultures and could, in fact, be universal to some degree. As the authors have previously clarified, neither of the prediction models derived for either sample represent a "perfect solution" to the problem of contraband concealment detection from stand-off. Most critically, the prediction models identified in these efforts will misclassify a minimum of one-in-five individuals (~20%) making it impractical as a stand-alone solution or comprehensive decision metric. Additionally, while the prediction models demonstrated statistically significant performance for the identification of liars, it cannot be concluded that these models are specifically identifying persons concealing dangerous firearms. For example, it is possible that the observed changes in whole-body movement are associated only with the psychosomatic influence of deception, and that an individual would be just as likely to be flagged if they were to attempt to smuggle some other contraband item (e.g. drugs) through an ECP. In such an eventuality, predictive algorithms would be identifying deceptive individuals representing extremely varying degrees of immediate threat to the ECP personnel. It would be clearly imprudent and unethical to suggest that the performance results presented in this report are sufficient to warrant such prediction models serving as the basis for lethal engagement in an ECP scenario. Rather, such algorithms, if further developed and demonstrated to be effective in-concert, may serve as a useful tool for flagging potential threats and reducing the load on personnel responsible for particularly high-volume ECPs. They are, however, at present susceptible to a relatively large degree of error.

Other limitations to the application of these findings involve both the sensors utilized in the present study and the testing environment. For example, the 3D motion analysis data were obtained using a high-resolution motion tracking system with sub-millimeter accuracy. Such spatial resolution is not available with 2D video technologies given current operational specifications (i.e. the demand for greater standoff distances may only allow for spatial

resolutions on the order of inches or even feet). Further, the motion tracking system employed in the current study was not challenged by changing environmental conditions such as low or altered lighting, occlusions, limited aspect angles, etc. It is reasonable to assume that deception prediction performance may degrade significantly as operational and/or environmental conditions interfere with sensor function.

These findings demonstrate the potential for intention-based information to be observed from whole-body movements. This is, however, entirely distinct from the notion that such a prediction model could be implemented in-field. Future work is required to determine if a) such movement signatures are universal across additional human cultures/populations, b) whether fieldable sensor technologies exist or may be developed to observe such signatures with accuracy and reliability sufficient to predict deception in-concert, and c) whether natural human variance and altered emotional responses to real-life deception scenarios obviate the possibility that predictive human movement signatures may be reliably elicited by persons concealing small arms or other contraband.